Food Analytical Methods (2019) 12:2361–2382
https://doi.org/10.1007/s12161-019-01573-w

Recent Progress in Rapid Analyses of Vitamins, Phenolic, and Volatile Compounds in Foods Using Vibrational Spectroscopy Combined with Chemometrics: a Review

Haroon Elrasheid Tahir[1] · Zou Xiaobo[1] · Xiao Jianbo[2] · Gustav Komla Mahunu[3] · Shi Jiyong[1] · Jun-Li Xu[4] · Da-Wen Sun[4]

Received: 1 February 2019 / Accepted: 19 June 2019 / Published online: 13 July 2019

Abstract

Nowadays, progresses in data processing software have promoted the application of infrared (e.g., FT-IR, NIR, MIR), Raman, and hyperspectral imaging (HSI) techniques for quantitative analysis of biological material and/or aroma compounds in foods. In this review, applications of vibrational spectroscopy combined with chemometrics are summarized including analysis of total polyphenol, individual polyphenols, vitamins, and aromatic compounds in raw and some processed products. Laboratory-based and online application of vibrational spectroscopies monitoring for analysis of phenolic compounds have been described. In addition, technical challenges and future trends have been covered. Based on the literature, the near-infrared technique often has an advantage over other spectroscopy approaches and the expensive and time-consuming chemical methods such as high-performance liquid chromatography and gas chromatography. Overall, the current review suggests that vibrational spectroscopies are promising and powerful techniques that can be used for rapid and accurate determinations of food nutraceuticals and volatile compounds in both academic and industrial contexts.

Keywords Food · Infrared spectroscopy · Raman spectroscopy · Hyperspectral imaging technique · Phenolic compounds · Volatile compound

Introduction

Polyphenol compounds and vitamins in food are of great interest and have gained more attention in recent years due to their health properties. Several epidemiological studies proved that these compounds have the capability to improve health by reducing risk or the symptom of chronic diseases (Shahidi and Zhong 2015). Recently, the role of flavor compounds in human health due to their antioxidant, anti-inflammatory, anti-cancer, and anti-obesity activities was reviewed by Ayseli and İpek Ayseli (2016). Minor constituents of food, especially phenolic and volatile compounds, are inherently associated with the global quality and positive sensory attributes of various foods (Inarejos-García et al. 2013). Typically, the price and ranking (i.e., high, medium, or low commercial value) of many foods depend on the organoleptic properties (Bianchi et al. 2005; D'Amico et al. 2016). Several attempts have been made to establish highly sensitive and selective approaches for measurement of bioactive and aroma components where comprehensive researches have been performed on the various extraction and separation techniques (e.g., SPE, SPME) as well as enhancing the chromatographic used (e.g., HPLC, GC-MS) (Tahir et al. 2016c; Tahir et al. 2017). Although these techniques can deliver accurate results, these methods are time-consuming, laborious, expensive, and complex (Cigic and Prosen 2009). Furthermore, the extraction process used may affect the chemical composition of phenolic compounds and/or aroma compounds (Boido et al. 2013; Bureau et al. 2019; Tahir et al. 2016a, b, c). Therefore, scientists continue to make significant attempts to find alternative rapid, ease-of-

✉ Zou Xiaobo
zou_xiaobo@ujs.edu.cn

[1] School of Food and Biological Engineering, Jiangsu University, 301 Xuefu Rd, Zhenjiang 212013, Jiangsu, China

[2] Institute of Chinese Medical Sciences, State Key Laboratory of Quality Research in Chinese Medicine, University of Macau, Taipa, Macau

[3] Department of Food Science & Technology, Faculty of Agriculture, University for Development Studies, Tamale, Ghana

[4] Food Refrigeration and Computerized Food Technology (FRCFT), School of Biosystems and Food Engineering, University College Dublin, National University of Ireland, Belfield, Dublin 4, Ireland

use, no or minimal sample preparation, and cost-effective techniques that might complement or replace conventional analytical tools in terms of measurement of aroma and bioactive compounds (Tahir et al. 2016a, c, 2017). Vibrational spectroscopies including infrared (e.g., FT-IR, NIR, MIR), Raman, and hyperspectral imaging (HSI) coupled with chemometric methods could be used as alternatives for quantitative analysis of various biologically active materials and aroma compounds (Fig. 1) in foods due to many advantages (Table 1). Some of these advantages include the hastening of the analysis and reducing the cost.

Nowadays, vibrational spectroscopies have been applied as powerful tools to study molecules, aromatic, and biological compounds in food (de Toledo et al. 2012; Li et al. 2019; Sekine et al. 2011). The contribution of these compounds (e.g., chlorogenic acid, flavonoid 3-methoxyquercetin, luteolin, phenol, pigments, tannin) to FT-IR, NIR, and Raman spectroscopy data has been previously reported (Coates 2000; Eravuchira et al. 2012; Marrassini et al. 2015; Sekine et al. 2011; Tahir et al. 2017; Tondi and Petutschnigg 2015). The infrared (IR) region includes that part of the electromagnetic spectrum in the wavelength range between 780 and 100,000 nm and is divided into near-IR, mid-IR, and far-IR subregions (Baeten and Dardenne 2002; Osborne 2006); the NIR region covers the wavelength range from 780 to 2500 nm (Osborne 2006). When compared with spectra collected in the mid-infrared (MIR) region, a NIR spectrum normally exhibits few well-defined, sharp peaks (Williams and Stevensen 1990). NIR technique operates with a light source from which the sample absorbs specific frequencies corresponding to overtones and combination bands of vibrational transitions of the molecule primarily of OH, CH, NH, and CO groups (Karoui 2018). MIR spectroscopy is typically used to determine the molecular composition of a sample. Raman technique is fundamentally similar to infrared since it gives information about the chemical bonds within the organic matrix. Raman technique is based on a special phenomenon termed Raman scattering. When the incident light is directed at a sample, a small fraction of the light is scattered by the sample. The scattered light conveys information on the vibrational band energies of molecules. A plot of the intensities of the scattered portion of incident light against the shifts in the frequency between the incident and the scattered light is known as Raman spectra (Kizil and Irudayaraj 2018). After vibrational spectroscopy data obtained, chemometrics techniques are employed to extract relevant information and remove the irrelevant information in order to determine volatile compounds and other bioactive compounds accurately. Generally, chemometrics comprises two parts, spectral preprocesses and regression methods. In the current article, a comprehensive overview of applications of four technologies for evaluating bioactive and volatile compounds will be

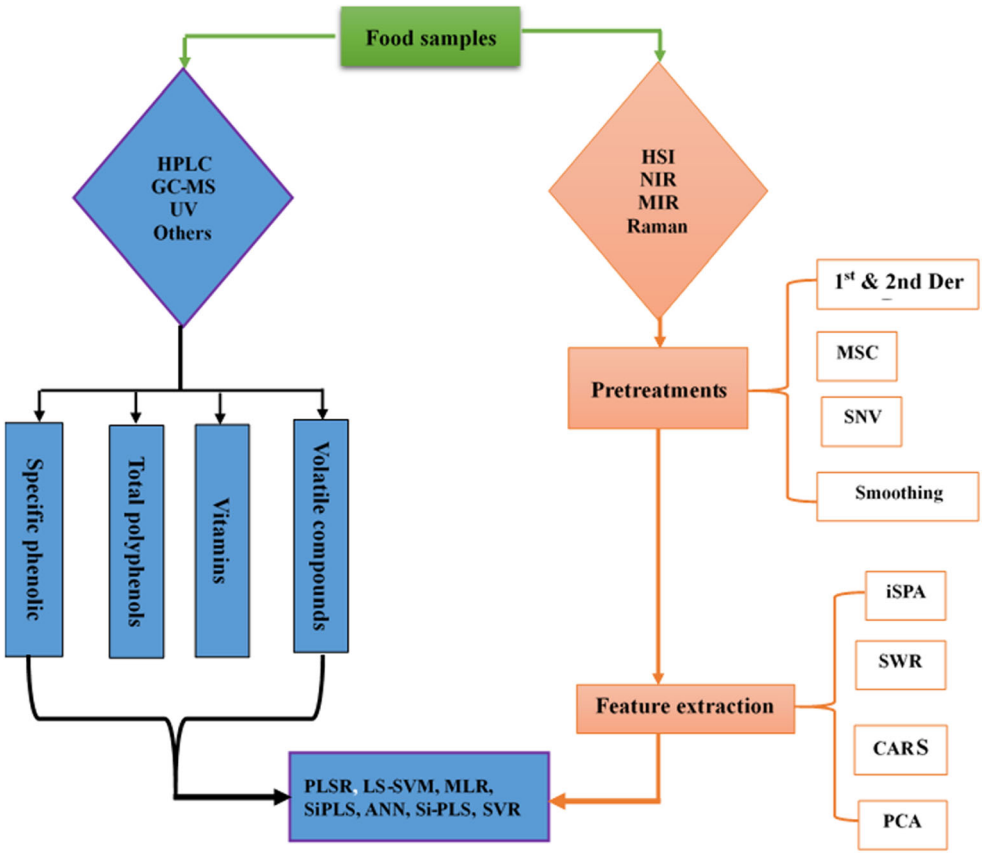

Fig. 1. The flowchart of assessing bioactive components volatile compound and antioxidant activity by vibrational spectroscopy

Table 1 The main features of some vibrational spectroscopy techniques for measurement of bioactive compounds and volatile in foods

Features	IR spectroscopy	NIR	Raman
Speed	Fast	Fast	Fast
Penetration depth	Several mm–several cm	Several mm–several cm	Several mm–several cm
Emission process	na	na	✓
Fluorescence-free spectra	na	na	✓
Low-frequency modes	Fair	na	Excellent
Best vibrations	Asymmetric	Comb/overtone	Symmetric
Process monitoring	✓	✓	✓
Saving of labor and reduction of samples to analyze	✓	✓	✓
Direct, non-invasive and non-destructive in situ analysis	✓	✓	✓
Compatible with suitable fiber optics	✓	✓	✓
Low-frequency modes	Fair	na	Excellent
Analyte	Component, active ingredients, physical attributes	Component, active ingredients, physical attributes	Component, active ingredients, physical attributes
Ease of sample preparation	Variable	Simple	Very simple
Intensity proportional to concentration	na	na	✓
Simple analysis: concentration vs peak area	✓	✓	✓
Analysis of liquids	Very simple	Very simple	Very simple
Analysis of powders	Simple	Simple	Very simple
Analysis of polymers	Simple	Simple	Very simple
Analysis of gases/volatile	Very simple	Simple	Simple
Qualitative and quantitative analysis	✓	✓	✓
Cost (price)	Moderate	Moderate to high	High
Application modes	Lab, portable, commercial	Lab, portable	Lab, portable

Not applicable (na)

addressed and some technical challenges and future research trends will be discussed as well.

Vibrational Spectroscopy

Recently, vibrational spectroscopy–based approaches have been extensively applied for the determination of various biologically active agents and volatile compounds in foods. These techniques, representing good alternatives to conventional methods, involve the application of toxic chemical and/or complicated sample preparations. Furthermore, vibrational spectroscopy methods enable the measurement of several characteristics from a single analysis in a very short time. Moreover, modern advancement in instrumentation and computational fields, as well as development in chemometric techniques, makes vibrational spectroscopy methods available for in situ and online investigation of different kinds of samples. Three key techniques are implemented to measure molecular vibrational motions: infrared spectroscopy (near and mid-infrared), Raman spectroscopy, and hyperspectral imaging system (HSI) technique.

The intense and specific bands indicated in the Raman, MIR, and FT-IR spectra data make these technologies very interesting, enabling the measurement of quality parameters in foods. MIR and NIR spectroscopies have a good signal intensity compared with Raman technique; however, MIR has the advantage over NIR; thus, trace components can be identified. The typical detection results of optical techniques are presented in Fig. 2 by taking honey and cocoa bean as an example (Caporaso et al. 2018; Tahir et al. 2017).

Infrared Spectroscopy

Infrared (IR) is a region that presents the molecular bond vibrations, in the spectral zones between 14,000 and 4000 cm^{-1} for NIR and 4000–400 cm^{-1} for MIR, offering valuable information regarding physical and chemical characteristics of samples. NIR spectrum results from complex overtones and combinations of tones whereas the MIR spectrum represents the fundamental vibrations of molecules (Burns and Ciurczak 2001; Ozaki, McClure et al. 2006). The suitable mode of infrared spectroscopy analysis mode should be determined based on the optical characteristics of the food samples (Fig. 3).

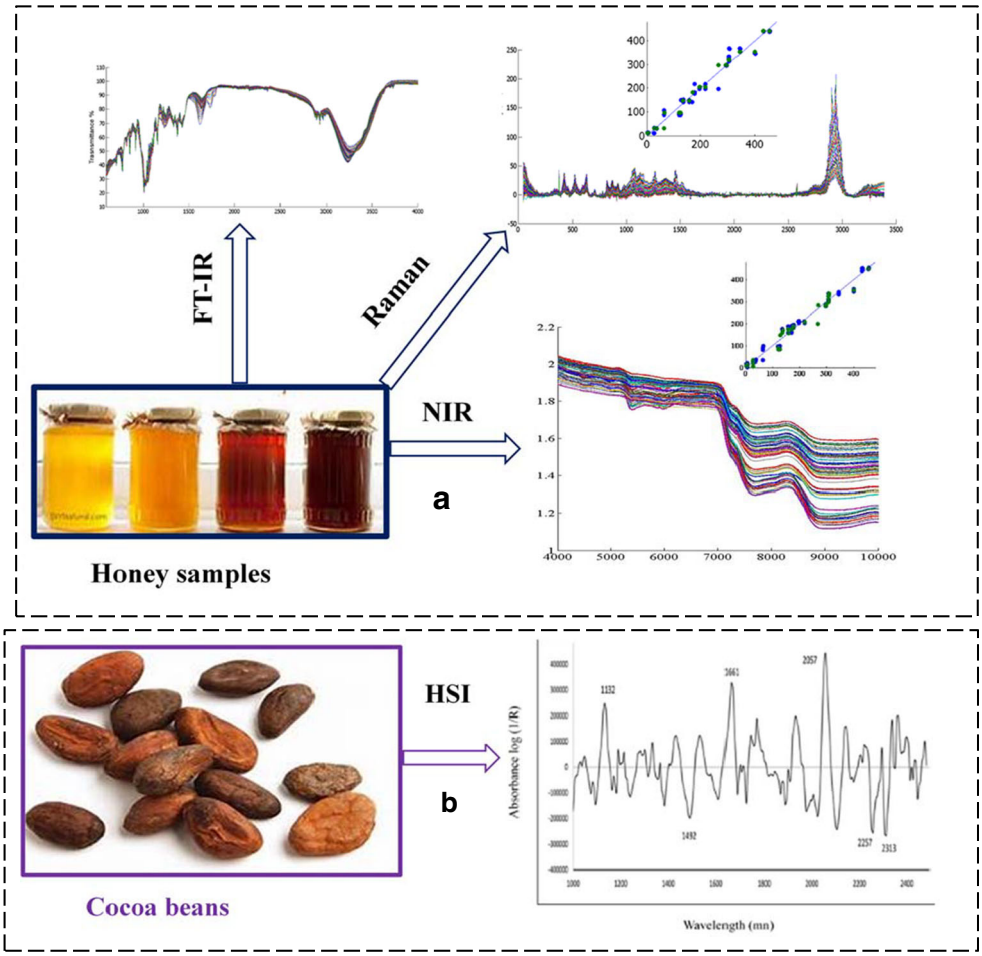

Fig. 2 (a) representative FT-IR, Raman, and NIR spectra of honey. (b) HSI spectra of cocoa Q4 beans

Reflectance mode determination is the easiest to acquire because it can be performing without contact with the food besides light intensities are fairly high. However, it is subjected to variations in surface characteristics. The advantage of the transmission cell is that it offers very accurate and reproducible spectroscopic determinations; however, the main drawbacks often require a destructive preparation or semi-preparation of the sample. Generally, transmission mode determinations are better than reflectance mode for measurements of internal disorders of foods. However, the intensity of light penetrating the food is often very low, making it a challenge to acquire accurate transmission determination, mainly in environments of high ambient light levels.

Transparent foods are usually analyzed in transmittance (Fig. 3a). Solid and semi-solid or turbid foods could be analyzed in diffuse transmittance (Fig. 3b), diffuse reflectance (Fig. 3c), or transflectance (*D*) based on their absorption and scattering properties. Also, pseudo absorbance (*A*) relative to standard reference material is determined ($A = \log(1/T)$ for transmittance and $\log(1/R)$ for reflectance spectra) (Reich 2005).

Raman Spectroscopy

In Raman spectroscopy, the sample is illuminated with a monochromatic laser beam which interacts with the molecules of the sample and creates a scattered light. The scattered light having a frequency different from that of incident light (inelastic scattering) is used to produce a Raman spectrum (Bumbrah and Sharma 2016; Skoog et al. 2017; Smith and Dent 2019). Raman spectroscopy also provides information regarding the chemical bonds within a compound similar to those obtained from infrared spectroscopy. However, the laser sources used in Raman technique might cause fluorescence of some organic molecule compounds, affecting the signal-to-noise ratio and decreasing the sensitivity of this technique. Hence, in many studies, it was used as a complement to IR data (Gao et al. 2018).

HSI Technique

Hyperspectral imaging (HSI) is a spectral imaging acquisition, which combines the main characteristics of spectroscopic and computer vision technique. It is considered a very efficient

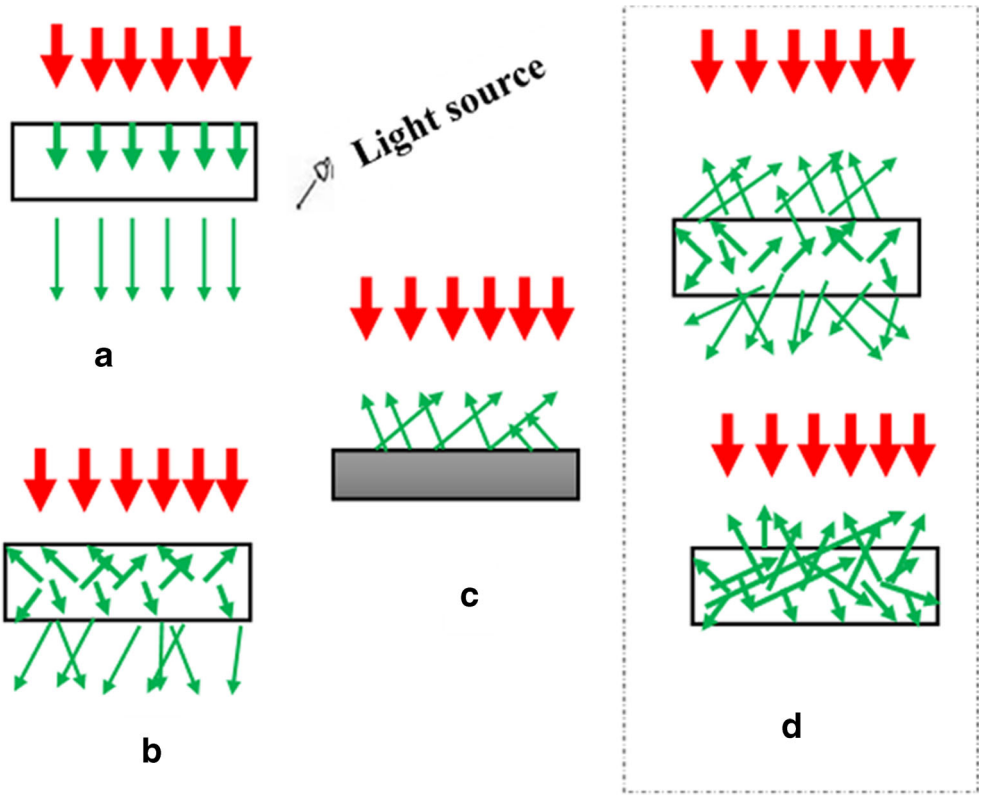

Fig. 3 Infrared spectroscopy assessment modes—**a** transmittance, **b** diffuse transmittance, **c** diffuse reflectance, and **d** transflectance

analytical tool to meet the growing demand of both spatial and spectral information, and therefore it has been extensively used for food quality and safety inspection (Su and Sun 2018a, b). HSI technique recorded spectral information in different spectral regions and can be combined with various spectroscopies such as VIS/NIR, MIR, and Raman (Pallone et al. 2018; Su and Sun 2018a, b). VIS/NIR HSI systems are the most common for food quality and safety measurements (Cheng et al. 2017). Over the past 6 years, vibrational spectroscopic technologies, particularly NIR, FT-IR, Raman, and NIR-HSI techniques, have demonstrated their potential in the measurement of food quality parameters including biologically active materials and volatile profiles.

Some Advantages and Drawbacks of Raman and Infrared Spectroscopies

Raman and IR spectroscopies showed many advantages that make these technologies attractive as substitutions to conventional, boring, and more time-consuming analytical methodologies. They are fast, do not require chemical reagents, and are non-destructive. Both Raman and IR spectroscopic procedures are integral because of their diverse determination rules. Since infrared motion needs a change in the dipole moment of a molecule, those bonds which are highly polar will absorb the most strong, for instance, C=O and O–H. Conversely, diatomic atoms, for example, H2, will not be infrared active (Pavia and Lampman 1996). In Raman spectroscopy, it is the change in polarizability, which is critical, and thus, bonds such as C=C are the most intense. Since all of the frequencies are determined simultaneously, most measurements by IR are made in a matter of seconds rather than several minutes. For instance, the detectors utilized in FT-IR are very sensitive and the optical throughput is greatly higher, which results in very lower noise levels; and the rapid scans enable the addition of several scans (i.e., signal averaging) to decrease the random measurement noise to any required level. In FT-IR spectroscopy, the moving mirror in the interferometer is the only continuously moving part. Therefore, there is very little risk of a mechanical breakdown. FT-IR system uses a HeNe laser, as an internal wavelength calibration standard, thus, does not require to be calibrated by the user. These advantages together with others make assessments conducted by FT-IR very accurate and reproducible. The main disadvantage of FT-IR is a single beam whereas dispersive techniques commonly have a double beam (Dutta 2017).

The main advantages of NIR spectroscopy over other spectroscopies are that they can provide spectra with high intensity, high resolution, precise spectral frequency measurement, being fluorescence-free, and ease of sample presentation. Furthermore, this technique is appropriate for online and in-line process monitoring and quality control of food products. Conversely, this system is characterized by poorly resolved spectra, the lack of information from nonpolar groups, an

absence of structural selectivity and sensitivity, and spectra affected by temperature changes (Fernández Pierna et al. 2018). NIR-HSI is widely used for measurements of bioactive compounds in food (Table 2). The advantage of NIR-HSI is the larger surface area being analyzed. In addition, it can acquire multi-constituent information and sensitive to minor chemical components. The main drawback of NIR-HSI is expensive and requires training (Jha 2010).

Raman spectra are obtained in a fairly fast acquisition time (milliseconds to minutes, depending on the sample). This enables for high-spatial-resolution 2D and 3D Raman mapping with tens of thousands of points being acquired in a few hours or less (Erasmus and Comins 2018). Also, in this technique, there is the absence of interference from overlapping peaks and, e.g., aqueous solutions do not present a problem (compared to, e.g., IR spectroscopy) (Alajtal 2010). In comparison with IR spectroscopy, one of the most attractive features of Raman techniques results from its weaker water interference. Thus, Raman technique can suitably analyze samples in various states (e.g., dried, hydrated, liquid, or solid state) with less sample preparation processes, which is fundamental for fast and non-destructive determination of the chemical composition of food in situ. Also, in this technique, fluorescence effect is well circumvented in the measurements and samples retained in glass bottles or simply in the raw form can be analyzed easily (Kizil and Irudayaraj 2018). A further advantage is that a Raman spectrum covers the spectral range between 4000 and ~ 100 cm^{-1}, depending on how effective the Rayleigh line filtering is (Y.-S. Li and Church 2014). Conversely, the acquisition of an IR spectrum over this frequency range depends on the utilization of both mid- and far-IR spectrometers. The main drawback with conventional Raman spectroscopy is the small scattering cross-section of many materials. The details of the advantages and drawbacks of infrared and Raman spectroscopy can be found in the literature (Baeten and Dardenne 2002; Y.-S. Li and Church 2014).

Chemometric Analysis

Nowadays, the research activities in chemometrics are very intense and a large number of publications dealing with the vibrational spectroscopy focus on this field. IR, Raman, and HSI are capable of providing useful information about the various characteristics of a sample. In addition to the sample properties, some redundant information originating from instrumental noise, scattering, and environmental effects might contribute to the complexity of a spectrum. These effects can be largely reduced by applying pretreatment techniques such as smoothing, standard normal variate (SNV), multiplicative signal correction (MSC), first derivative (1st Der), and second derivative (2nd Der) (Mora-Ruiz et al. 2017; Pu et al. 2015; Tahir et al. 2016a).

Due to the large overlap and the complex nature of continuous data, sometimes, it is a challenge to find the positions of characteristic bands that represent the different components in plant foods. To avoid using irrelevant information, the selection of feature wavelengths in the vibrational spectroscopy (e.g., HSI and NIR) region is a highly effective method to develop a robust and accurate model (Table 2) (Su and Sun 2018a, b). Thus, different combinations of feature wavelengths associated with specific quality parameters are expected to be efficiently captured. Several wavelength selection procedures such as successive projection algorithm (SPA) and stepwise regression (SWR) (Y.-C. Yang et al. 2015), interval selection in partial least squares (iSPA) (Mariani et al. 2015). competitive adaptive reweighted sampling (CARS) (Ma et al. 2016), and principal component analysis (PCA) (Khulal et al. 2016) have been employed over the last couple of decades. The most common modeling techniques for quantitative analysis of volatile and bioactive compounds include partial least squares regression (PLSR), least squares-support vector machine (LS-SVM), modified linear regression (MLS), artificial neural network (ANN), synergy interval partial least square regression (Si-PLS), support vector regression (SVR), and backward interval partial least squares (bi-PLS) (Table 2). Generally, a good regression model is characterized by higher coefficients in calibration (R_c), cross-validation (R_{cv}), and prediction (R_p) and lower error values in calibration (RMSEC), cross-validation (RMSECV), prediction (RMSEP), standard error of prediction (SEP), and standard error of calibration (SEC).

Applications on Volatile and Bioactive Components

The under-mentioned sections summarized the recent progress of the applications of spectroscopic techniques with suitable chemometrics methods in this field (Table 2 and Table 3). Generally, the applications of these techniques can be grouped into the following categories: (1) measurement of volatile compounds, (2) measurement of individual bioactive compounds, (3) measurement of a group of bioactive compounds. HSI was mostly used for (3), and Raman and MIR for categories (2) and (3), while NIR has been applied for all categories.

Basically, determination of phytochemical compounds and vitamins using Raman, NIR, MIR, and HSI techniques requires appropriate reference chemical assays to be performed simultaneously as spectral measurements. Spectroscopic techniques are indirect tools for measuring volatile compounds and health-related components in foods. Conventional methods such as GC-MS, HPLC, and UV-vis spectrophotometer are usually performed to obtain data about volatile and bioactive compounds (such as vitamins, phenolics, and

Table 2 Applications of NIR spectroscopy, FT-IR spectroscopy, Raman spectroscopy, and HSI technique for bioactive compound assessments of various food products

Food items	Parameters	Quantification	Module	Wavelength range	Optimal model	Accuracy	References
Raw propolis	TPC (mg GAE g^{-1}) TFC (mg QE g^{-1})	UV	NIR	1100–2000 nm	MPLS	R^2_p = 0.97, SECV = 22,26, RMSEP = 9.03 R^2_p = 0.96, SECV = 7.28, RMSEP = 3.24	(Revilla et al. 2017)
Olive oil	α-Tocopherols (ppm) β-Tocopherols (ppm)	HPLC/FLD	NIR	350–1000 nm	PLS	R_p = 0.91, SEC = 36.14, SEP = 47.21 R_p = 0.41, SEC = 0.59 , SEP = 1.32	(Cayuela and García 2017)
	γ-Tocopherol (ppm)					R_p = 0.88, SEC = 5.34 , SEP = 6.33	
	Total tocopherols (ppm)					R_p = 0.90, SEC = 57.15 , SEP = 61.84	
Guava nectar Cashew fruit	Ascorbic acid (mg100 g^{-1}) Ascorbic acid (mg 100 g^{-1})	Titrimetric	NIR	10,000 to 4000 cm^{-1}	MPLS	R^2_p = 0.86, RMSEC = 6.41, RMSEP = 7.40 R^2_p = 0.84, RMSEC = 4.60 , RMSEP = 4.80	(Caramês et al. 2017a)
Honey	TFC (mg QE 100 g^{-1}) TPC (mg GAE 100 g^{-1})	UV-visible	NIR	10,000–4000 cm^{-1}	PLS	R_p = 0.95, RMSECV = 0.92, RMSEP = 1.01 R_p = 0.94, RMSECV = 13.60, RMSEP = 14.50	(Tahir, Xiaobo, Tinting, et al., 2016)
	Total carotenoid (mg kg^{-1})					R_p = 0.96, RMSECV = 0.34 , RMSEP = 0.35	
Spent coffee	Caffeic acid (mg kg^{-1}) (+)-Catechin (mg kg^{-1})	HPLC-PDA	FT-NIR	10,000–4000 cm^{-1}	PLS	R^2_p = 0.92, RMSECV = 34.0, RMSEP = 32.4 R^2_p = 0.88, RMSECV = 4.50, RMSEP = 4.40	(Magalhães et al. 2016)
	Chlorogenic acid (mg kg^{-1})					R^2_p = 0.71, RMSECV = 300.00, RMSEP = 352.00	
Okra seeds	TPC (%) Isoquercitrin (%)	UV-visible HPLC-UV	FT-MIR FT-MIR	2,000–4000 cm^{-1} 2,000–4000 cm^{-1}	PLS PLS	R^2_p = 0.97, RMSECV = 0.39, RMSEP = 0.34 R^2_p = 0.90, RMSEC = 0.03, RMSEP = 0.02	(Xia et al. 2018)
	Quercetin-3-*O*-gentiobioside (%)					R^2_p = 0.94, RMSECV = 0.09, RMSEP = 0.05	
Wine grape	Anthocyanin (CGE, mg g^{-1})	UV-vis	HSI	900–1700 nm	PLS	R^2_p = 0.97, RMSEC = 0.00, RMSEP = 0.012	(Zhang et al. 2017)
Apple	TPC (GAE mg kg^{-1}) TFC (GAE m kg^{-1})	UV-vis	FT-NIR	12,500–3600 cm^{-1}	PLS	R^2_p = 0.92, RMSECV = 54.00 R^2_p = 0.86, RMSECV = 23.00	(Giovanelli et al. 2014)
Red cabbage	T. anthocyanins (mg L^{-1}) TAC (mg L^{-1})	UV-vis	FT-IR-ATR?	4000–650 cm^{-1}	PLS	R_p = 0.99, RMSECV = 18.06, RMSEP = 18.40 R_p = 0.96, RMSECV = 21.25, RMSEP = 13.93	(I. R. N. de Oliveira et al. 2018)
	TPC (mg GAE L^{-1})					R_p = 0.99, RMSECV = 44.41, RMSEP = 42.46	
Red cabbage	T. anthocyanins (mg L^{-1}) Monomeric anthocyanins (mg L^{-1})	UV-vis	NIR	10000–4000 cm^{-1}	PLS	R_p = 0.99, RMSECV = 16.35, RMSEP = 10.74 R_p = 0.99, RMSECV = 20.15, RMSEP = 19.34	(I. R. N. de Oliveira et al. 2018)
	TPC (mg GAE L^{-1})					R_p = 0.99, RMSECV = 42.68, RMSEP = 35.96	
Squash fruit flesh	Total carotenoid (mg kg^{-1}) Lutein (mg kg^{-1})	UV-vis HPLC	NIR NIR	400–2500 nm 400–2500 nm	MPLS MPLS	R^2_p = 0.95, SEP = 31.70 R^2_p = 0.96, SEP = 26.80	(Martínez-Valdivieso et al. 2014)
	β-Carotene (mg kg^{-1})					R^2_p = 0.81, SEP = 2.27	
Dehydrated tomato	Lycopene (mg lycopene/kg) TPC (g citric acid 100 g^{-1})	UV-vis	NIR	800–2500 nm	RBF-NN	R_p = 0.94, RMSEC = 9.74 , RMSEP = 16.10 R_p = 0.95, RMSEC = 0.04, RMSEP = 0.08	(Ding et al. 2016)
Mint tea	TPC (g GAE100 g^{-1}) TFC (g rutin 100 g^{-1})	UV-vis	NIR	800–2500 nm	LS-SVM	R_p = 0.98, RMSEC = 0.04, RMSEP = 0.11 R_p = 0.98, RMSEC = 0.07, RMSEP = 0.14	(Dong et al. 2014)
Hawthorn fruit	TPC (g GAE100g^{-1})	UV-vis	NIR	800–2500 nm	LS-SVM	R_p = 0.95, RMSEC = 0.09, RMSEP = 0.14	(Dong et al. 2013)
Pomegranate juice	TPC (g GAE L^{-1}) TAC (g CGE L^{-1})	UV-vis	MIR	5000–930 nm	PLS	R^2_p = 0.682, RMSEE = 0.13, RMSEP = 0.15 R^2_p = 0.74, RMSEE = 0.13, RMSEP = 0.21	(Arendse et al. 2018)
	Ascorbic acid (g AAE L^{-1})					R^2_p = 0.71, RMSEE = 0.09, RMSEP = 0.11	

Table 2 (continued)

Food items	Parameters	Quantification	Module	Wavelength range	Optimal model	Accuracy	References
Roasted coffee	Chlorogenic acid (%)	HPLC-UV	NIR	1000–2700 nm	PLS	R^2_p = 0.76, RMSECV = 1.10	(Shan et al. 2014)
Red grape	TPC (mg GAE g^{-1})	UV-vis	HSI	900–1700 nm	MPLS	R^2_p = 0.89, SECV = 1.07,	(Nogales-Bueno et al. 2014)
Red wine	Trans-resveratrol (mg L^{-1})) Quercetin (mg L^{-1})	HPLC/DAD	NIR	190–2500 nm	PLS	R^2val = 0.87, RMSECV = 0.36 R^2val = 0.87, RMSEC = 0.61	(Martelo-Vidal and Vázquez 2014)
	Catechin (mg L^{-1})					R^2val = 0.89, RMSEC = 0.65	
	Malvin (mg L^{-1})					R^2val = 0.76, RMSEC = 0.55	
	Epicatechin (mg L^{-1})					R^2val = 0.87, RMSEC = 0.73	
	Oenin (mg L^{-1})					R^2val = 0.97, RMSEC = 0.62	
	Syringic acid (mg L^{-1})					R^2val = 0.98, RMSEC = 0.63	
Grape juice	TAC (mg CGE 100 mL^{-1}) TPC (mg GAE100 mL^{-1})	UV-vis	FT-MIR	4000–400 cm^{-1}	PLS	R^2C = 0.81, RMSEC = 4.31, RMSEP = 4.22 R^2_p = 0.90, RMSEC = 0.26 , RMSEP = 0.21	(Caramês et al. 2017b)
Pomegranate fruit	TPC (g GAE L^{-1}) TAC (g CGE (g L^{-1})	UV-vis	FT-NIR	1064–1333 nm	PLS	R^2_p = 0.868, RMSEE = 0.11, RMSEP = 0.11 R^2_p = 0.71, RMSEE = 0.16, RMSEP = 0.13	(Arendse et al. 2017)
	Ascorbic acid (g L^{-1})					R^2_p = 0.854, RMSEE = 0.08, RMSEP = 0.09	
Yerba mate	TPC (mg GAE g^{-1})	UV-vis	NIR	10.000–4.000 cm^{-1}	PLS	R_p = 0.83, RMSECV = 16.07, RMSEP = 12.12	(Frizon et al. 2015)
Yerba mate	TPC (mg GAE g^{-1})	UV-vis	NIR	10.000–4.000 cm^{-1}	PLS	R_p = 0.83, RMSECV = 16.07, RMSEP = 12.12	(Frizon et al. 2015)
Apple	Ascorbic acid (mg AAE100 g^{-1}) TPC (μg g^{-1})	HPLC-UV UV-vis	NIR	400–2500 nm	LS-SVM	R^2_p = 0.80, SEC = 3.40, SEP = 4.90 R^2_p = 0.92, SEC = 178.00, SEP = 140.00	(Pissard et al. 2013)
Quinoa	Vitamin E (mg 100 g^{-1}) TPC (mg GAE g^{-1})	HPLC UV-vis	NIR	1100–2000 nm	MPLS	R^2_p = 0.86, SECV = 4.06 R^2_p = 0.96, SECV = 0.33	(Moncada et al. 2013)
Cocoa beans	TPC (mg FAE g^{-1})	UV-vis	HSI	1000–2500 nm	PLS	R^2_p = 0.70, RMSECV = 28.09, RMSEP = 34.13	(Caporaso et al. 2018)
Propolis	TFC (mg rutin g^{-1})	UV-vis	NIR	1100–2000 nm	MPLS	R^2_p = 0.63, SECV = 13.4, RMSEP = 9.50	(Betances-Salcedo et al. 2017)
Coffee beans	3-Caffeoylquinic acid (mg g^{-1}) 4-Caffeoylquinic acid (mg g^{-1})	HPLC-DAD	FT-IR	4000–400 cm^{-1}	PLS	R^2_p = 0.92, RMSECV = 0.36 R^2_p = 0.94, RMSECV = 0.48	(Liang et al. 2016)
	5-Caffeoylquinic acid (mg g^{-1})					R^2_p = 0.99, RMSECV = 1.55	
	3,5-Dicaffeoylquinic acid (mg g^{-1})					R^2_p = 0.96, RMSECV = 0.16	
	3,4-Dicaffeoylquinic acid (mg g^{-1})					R^2_p = 0.98, RMSECV = 0.21	
	4,5-Dicaffeoylquinic acid (mg g^{-1})					R^2_p = 0.98, RMSECV = 0.17	
Honey	Catechin (μg g^{-1}) Chlorogenic acid (μg g^{-1})	HPLC-DAD	FT-IR	4000–600 cm^{-1}	PLS	R^2_p = 0.99, RMSECV = 0.46, RMSEP = 0.40 R^2_p = 0.99, RMSECV = 0.44, RMSEP = 0.43	(Tahir et al. 2017)
	Syringic acid (μg g^{-1})					R^2_p = 0.99, RMSECV = 0.33, RMSEP = 1.00	
	Vanillic acid (μg g^{-1})					R^2_p = 0.95, RMSECV = 0.40, RMSEP = 0.45	
Honey	Catechin (μg g^{-1})	HPLC-DAD	Raman	50 to 3500 cm^{-1}	PLS	R^2_p = 0.99, RMSECV = 0.44, RMSEP = 0.41	

Table 2 (continued)

Food items	Parameters	Quantification	Module	Wavelength range	Optimal model	Accuracy	References
	Chlorogenic acid (μg g^{-1})					R^2_p = 0.99, RMSECV = 0.42, RMSEP = 0.33	
	Syringic acid (μg g^{-1})					R^2_p = 0.99, RMSECV = 0.41, RMSEP = 1.00	
	Vanillic acid (μg g^{-1})					R^2_p = 0.93, RMSECV = 0.40, RMSEP = 0.46	
Carrots	Carotenoids (μg g^{-1})	HPLC-DAD	FT-Raman	400–2500 nm	PLS	R^2_p = 0.96, RMSEC = 449, RMSEP = 476	(Krähmer et al. 2016)
	α-Carotene (μg g^{-1})					R^2_p = 0.97, RMSEC = 88.00, RMSEP = 166.00	
	β-Carotene (μg g^{-1})					R^2_p = 0.96, RMSEC = 158.00, RMSEP = 295.00	
	Lutein (μg g^{-1})					R^2_p = 0.80, RMSEC = 7.10, RMSEP = 11.50	
	Polyacetylenes (μg g^{-1})					R^2_p = 0.91, RMSEC = 125.00, RMSEP = 291.00	
	Falcarinol (μg g^{-1})					R^2_p = 0.36, RMSEC = 231.00, RMSEP = 264.00	
	Falcarindiol (μg g^{-1})					R^2_p = 0.90, RMSEC = 225.00, RMSEP = 271.00	
	3-*O*-Acetylfalcarindiol (μg g^{-1})					R^2_p = 0.66, RMSEC = 5.00, RMSEP = 10.20	
Chocolate	(-)-Epicatechin (mg GAE g^{-1})	HPLC-DAD	FT-IR	1800–700 cm^{-1}	PLS	R^2_p = 0.72, RMSECV = 0.58, RMSEP = 0.57	(Hu et al. 2016)
	(+)-Catechin (mg GAE g^{-1})					R^2_p = 0.86, RMSECV = 0.09, RMSEP = 0.10	
	TPC (mg GAE/g)	UV-vis	FT-IR	1800–700 cm^{-1}	PLS	R^2_p = 0.88, RMSECV = 4.21, RMSEP = 5.08	
Olive oil	Hydroxytyrosol (mg kg^{-1})	HPLC-DAD	FT-NIR	12,500–4000 cm^{-1}	PLS	R_p = 0.20, RMSECV = 4.49, RMSEP = 4.06	(Inarejos-García et al. 2013)
	Tyrosol (mg/kg)					R_p = 0.34, RMSECV = 6.60, RMSEP = 3.20	
	Hydroxytyrosol derivatives (mg kg^{-1})					R_p = 0.85, RMSECV = 32.90, RMSEP = 25.50	
	3,4-DHPEA-EDA (mg kg^{-1})					R_p = 0.83, RMSECV = 24.20, RMSEP = 19.10	
	3,4-DHPEA-EA (mg kg^{-1})					R_p = 0.68, RMSECV = 17.6 , RMSEP = 13.10	
	o-Diphenols (mg kg^{-1})					R_p = 0.85, RMSECV = 33.30, RMSEP = 26.30	
	Tyr derivatives (mg kg^{-1})					R_p = 0.57, RMSECV = 24.50 , RMSEP = 23.80	
	p-HPEA-EDA (mg/kg)					R_p = 0.41, RMSECV = 19.50, RMSEP = 20.40	
	p-HPEA-EA (mg/kg)					R_p = 0.62, RMSECV = 0.07, RMSEP = 0.06	
	Total phenols (mg/kg)					R_p = 0.79, RMSECV = 45.10, RMSEP = 44.50	
Propolis	TPC (mg EAG g^{-1})	UV-vis	FT-IR	4000–400 cm^{-1}	PLS	R^2_p = 0.71, RMSEC = 3.41, RMSEP = 9.15	(da Silva et al. 2018)
Wine grapes	TPC (g/L CE)	UV-vis	HSI	380–1028 nm	SVR	R^2_p = 0.91, RMSEC = 0.20, RMSEP = 0.18	
	TAC (g CGE L^{-1})					R^2_p = 0.88, RMSEC = 0.04, RMSEP = 0.14	(Zhang et al. 2017)
Chickpea	TPC (mg kg^{-1})	UV	FT-IR	4000–450 cm^{-1}	PLS	R^2_p = 0.95,RMSECV = 50.33	(Kadiroğlu et al. 2018)

Total phenolic content (TPC); total flavonoid content (TFC); total anthocyanins content (TAC); partial least squares (PLS); modified partial squares (MPLS); root mean square error of cross-validation (RMSECV); root mean square error of prediction (RMSEP); standard error of prediction (SEP); standard error of calibration (SEC); standard error of cross-validation (SECV); interval selection in partial least squares (iSPA-PLS); least squares-support vector machine (LS-SVM); support vector regression (SVR); radial basis function neural networks (RBF-NN); root mean square error of estimation (RMSEE); gallic acid equivalents (GAE); ascorbic acid equivalents (AAE); ferulic acid equivalent (FAE); catechin equivalents (CE); quercetin equivalent (QE); information not available(N/A); cyanidin-3-glucoside (CGE)

Table 3 Applications of IR spectroscopy, Raman spectroscopy, and HSI for volatile compounds evaluations of various food products

Food items	Parameters	Quantification	Module	Wavelength range	Optimal model	Accuracy	References
Olive oil	1-Penten-3-ol (mg kg^{-1})	GC-MS	FT-NIR	12,500–4000 cm^{-1}	PLS	R_p = 0.52, RMSECV = 0.09,	(Inarejos-García et al. 2013)
	1-Penten-3-ona (mg kg^{-1})					R_p = 0.57, RMSECV = 0.19, RMSEP = 0.20	
	C5 volatiles (mg kg^{-1})					R_p = 0.58, RMSECV = 0.25, RMSEP = 0.25	
	Hexanal (mg/kg)					R_p = 0.57, RMSECV = 0.13, RMSEP = 0.11	
	E-2-hexenal (mg kg^{-1})					R_p = 0.42, RMSECV = 0.99, RMSEP = 1.06	
	C6 aldehydes (mg kg^{-1})					R_p = 0.43, RMSECV = 1.10, RMSEP = 1.14	
	Hexanol (mg kg^{-1})					R_p = 0.62, RMSECV = 0.14, RMSEP = 0.11	
	Z-3-hexenol (mg kg^{-1})					R_p = 0.59, RMSECV = 0.58, RMSEP = 0.67	
	E-2-hexenol (mg kg^{-1})					R_p = 0.51, RMSECV = 0.19, RMSEP = 0.16	
	C6 alcohols (mg/kg)					R_p = 0.56, RMSECV = 0.78, RMSEP = 0.83	
	2-Methylbutanal (mg kg^{-1})					R_p = 0.71, RMSECV = 0.04, RMSEP = 0.05	
	3-Methylbutanal (mg kg^{-1})					R_p = 0.67, RMSECV = 0.04, RMSEP = 0.05	
Lavender lavandin oils	Eucalyptol	GC-MS	NIR	4000 to 10,000 cm^{-1}	PLS	R^2_p = 0.98, SEC = 0.38, SEP = 0.44	(Lafhal et al. 2016)
	Trans-β-ocimene (%)					R^2_p = 0.99, SEC = 0.43, SEP = 0.36	
	Linalool (%)					R^2_p = 0.99, SEC = 0.98, SEP = 0.85	
	Camphor (%)					R^2_p = 0.99, SEC = 0.19, SEP = 0.23	
	Borneol (%)					R^2_p = 0.99, SEC = 0.17, SEP = 0.20	
	Linalyl acetate (%)					R^2_p = 0.99, SEC = 0.78, SEP = 0.82	
	Lavandulyl acetate (%)					R^2_p = 0.97, SEC = 0.31, SEP = 0.42	
	β-Caryophyllene (%)					R^2_p = 0.99, SEC = 0.25, SEP = 0.28	
Red wine	2,4,6-Trichloroanisole (%)	GC-MS	NIR	10000-4000 cm^{-1}	PLS	R^2_p = 0.75, SEC = 17.29, SEP = 18.42	(Garde-Cerdán et al. 2012)
	2,3,4,6-Tetrachloroanisole (%)					R^2_p = 0.99, SEC = 25.27, SEP = 27.17	
	2,3,4,5,6-Pentachloroanisole (%)					R^2_p = 0.99, SEC = 10.12, SEP = 11.66	
	2,4,6-Trichlorophenol (%)					R^2_p = 0.83, SEC = 15.85, SEP = 16.34	
	2,4,6-Tribromoanisole (%)					R^2_p = 0.75, SEC = 27.51, SEP = 29.81	
Wine	Ethyl acetate (mg L^{-1})	GC-MS	NIR	5435–6357 cm^{-1}	PLS	R^2_p = 0.95, RMSE(%) = 7.60	(Genisheva et al. 2018)
	Methanol (mg L^{-1})					R^2_p = 0.96, RMSE(%) = 8.50	
	2-Methyl-1-butanol (mg L^{-1})					R^2_p = 0.98, RMSE(%) = 3.60	
	3-Methyl-1-butanol (mg L^{-1})					R^2_p = 0.98, RMSE(%) = 4.50	
	2-Phenylethanol (mg L^{-1})					R^2_p = 0.97, RMSE(%) = 4.80	
	3-Methylbutyl acetate (mg L^{-1})					R^2_p = 0.97, RMSE(%) = 23.00	
	Ethyl lactate (mg L^{-1})					R^2_p = 0.98, RMSE(%) = 5.90	
	Ethyl octanoate (mg L^{-1})					R^2_p = 0.95, RMSE(%) = 13.40	
	Diethyl succinate (mg L^{-1})					R^2_p = 0.97, RMSE(%) = 12.40	
	Diethyl malate (mg L^{-1})					R^2_p = 0.96, RMSE(%) = 14.50	
Apple wine	Alcohol (ml/L)	Alcoholmeter	NIR	6101.9–5446.2, 11,995.4–7498.1 cm^{-1}	PLS	R^2_p = 0.99, RMSECV = 4.63, RMSEP = 4.25	(Peng et al. 2016)
Aromatic plant	α-Terpinene (%)	GC-MS	NIR	1000–2500 nm	PLS	R^2_p = 0.97, RMSECV = 0.21 , RMSEP = 0.14	(Ercioglu et al. 2018)
	γ-Terpinene (%)					R^2_p = 0.96, RMSECV = 0.44, RMSEP = 0.24	
	Limonene (%)					R^2_p = 0.96, RMSECV = 1.29, RMSEP = 0.91	

Table 3 (continued)

Food items	Parameters	Quantification	Module	Wavelength range	Optimal model	Accuracy	References
	ρ-Cymene (%)					R^2_p = 0.97, RMSECV = 0.42, RMSEP = 0.23	
	Myrcene (%)					R^2_p = 0.99, RMSECV = 2.21, RMSEP = 1.64	
	α-Pinene (%)					R^2_p = 0.96, RMSECV = 2.31, RMSEP = 1.90	
	β-Pinene (%)					R^2_p = 0.96, RMSECV = 2.31, RMSEP = 1.90	
	Sabinene (%)					R^2_p = 0.97, RMSECV = 0.97, RMSEP = 0.38	
	Carene (%)					R^2_p = 0.96, RMSECV = 1.26 , RMSEP = 1.11	
	Camphene (%)					R^2_p = 0.97, RMSECV = 0.21, RMSEP = 0.19	
	Terpineol (%)					R^2_p = 0.97, RMSECV = 0.36, RMSEP = 0.84	
	Linalool (%)					R^2_p = 0.95, RMSECV = 4.14 , RMSEP = 2.83	
	Linalyl acetate (%)					R^2_p = 0.99, RMSECV = 0.90, RMSEP = 0.21	
	Borneol (%)					R^2_p = 0.96, RMSECV = 0.86 , RMSEP = 0.70	
	Methyl eugenol (%)					R^2_p = 0.96, RMSECV = 0.99, RMSEP = 0.70	
	Carvone (%)					R^2_p = 0.97, RMSECV = 7.93, RMSEP = 6.85	
	Camphor (%)					R^2_p = 0.98, RMSECV = 1.97, RMSEP = 1.28	
	Ar-curcumene (%)					R^2_p = 0.99, RMSECV = 2.06, RMSEP = 1.88	
	Eucalyptol (%)					R^2_p = 0.97, RMSECV = 6.37 , RMSEP = 4.63	
	Thymol (%)					R^2_p = 0.99, RMSECV = 0.27, RMSEP = 0.13	
	Carvacrol (%)					R^2_p = 0.99, RMSECV = 9.40 , RMSEP = 4.24	
Wine	Alcohol (%vol)	Densitometry	MIR	3010 to 950 cm^{-1}	PLS	R^2_p = 0.99, RMSECV = 0.08, RMSEP = 0.09	(Teixeira dos Santos et al. 2018)
	Alcohol (%vol)		NIR	9091–4003 cm^{-1}	PLS	R^2_p = 0.95, RMSECV = 0.33, RMSEP = 0.20	
	Alcohol (%vol)		Raman	3500 to 57 cm^{-1}	PLS	R^2_p = 0.91, RMSECV = 0.46, RMSEP = 0.37	
Cheese	Acetaldehyde (%)	GC-MS	NIR	100–2000 nm	MPLS	R^2_p = 0.79, SECV = 0.06	(González-Martín et al. 2014)
	Ethanol (%)					R^2_p = 0.86, SECV = 4.67	
	1-Propanol (%)					R^2_p = 0.69, SECV = 2.20	
	2-Butanol (%)					R^2_p = 0.73, SECV = 1.93	
	2-Pentanol (%)					R^2_p = 0.66, SECV = 0.32	
	3-Methyl-1-butanol (%)					R^2_p = 0.61, SECV = 0.07	
	2-Butanone (%)					R^2_p = 0.62, SECV = 0.38	
	2-Pentanone (%)					R^2_p = 0.71, SECV = 0.59	
	2-Heptanone (%)					R^2_p = 0.85, SECV = 0.30	
	2-Nonanone (%)					R^2_p = 0.90, SECV = 0.14	

Partial least squares (PLS); modified partial squares (MPLS); root mean square error (RMSE); back propagation artificial neural network (BPANN); root mean square error of cross-validation (RMSECV); root mean square error of prediction (RMSEP); standard error of prediction (SEP); standard error of calibration (SEC); standard error of cross-validation (SECV)

flavonoid). Thereafter, appropriate mathematic models might be developed for the determination of concentrations of either individual compound or prediction of total antioxidant compounds based on how models were developed.

Analysis of Total Phenolic Compounds

For predicting TPC using NIR, difference feature wavelengths were extracted using difference selection techniques. For example, competitive adaptive reweighted sampling-partial least square (CARS-PLS) was used to predict TPC in tea (Ma et al. 2016). Compared with the PLS model built from the whole wavelength, CARS-PLS algorithm can reduce the prediction error and enhance the correlation coefficients (R^2_p) from 0.8023 to 0.8412. The TPC in honey was determined using NIR reflectance (10,000–4000 cm^{-1}) combined with various pretreatments (such as baseline correction, SNV, MSC, and 1st Der). The results indicated that the raw data model was the most robust with a high correlation coefficient ($R_p = 0.94$) and a higher ratio of performance to the standard deviation (RPD < 3.50) which indicated the precision of NIR using spectra without any pretreatments (Tahir et al. b). NIR has also been successfully applied to obtain non-destructive measurements of TPC in many foods such as apples, red cabbage, and honey (Table 2). Based on the abovementioned studies, it can be concluded that it is possible to accurately determine TPC in foods using NIR technology. Furthermore, as presented in Fig. 4, NIR is the most effective and widespread technique for quantitative analysis of bioactive compounds in foods.

The online application of vibration spectroscopy techniques in the determination of bioactive compounds is limited. Aleixandre-Tudo et al. (2019) investigated the feasibility of online application NIR for measurement of bioactive compounds in intact and crushed grape berries transported on a conveyor belt system online (Fig. 5). The study was conducted using commercial cellar equipment, which makes this system valid for the commercial condition. The PLS results indicated that NIR technique is a powerful tool for prediction of the bioactive compounds such as phenolic compounds in wine-like and homogenate samples. The developed model showed lower prediction errors (RMSEP = 12.3%). The authors concluded that the result of this study could be implemented in fruit sorting and bench-marking as well as for decision-making reasons, before the fermentation procedure. However, comprehensive studies with a large number of samples with different maturity stages are required to demonstrate this.

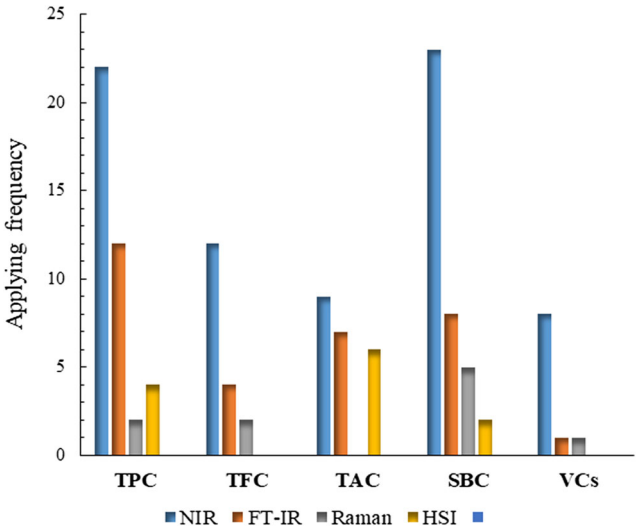

Fig. 4 Publication numbers of applying vibrational spectroscopy for measurements of total phenolic compound content (TPC), total flavonoid content (TFC), total anthocyanin content (TAC), total antioxidant activity (TAA), specific bioactive compound (SBC), and volatile compounds (VCs) in foods from July 2011 to January 2019

TPC in red cabbage was analyzed by NIR (10000–4000 cm^{-1}) and ATR-FT-IR (3600–3200 cm^{-1}) (I. R. N. de Oliveira et al. 2018). The authors applied ordered predictors selection (OPS) and genetic algorithm (GA) for feature extraction prior to developing the PLS model. The results indicated that PLS combined with the OPS algorithm had better performance (RMSECV = 44.41 mg gallic acid equivalents (GAE) 100 g^{-1}) (RMSEP = 42.46 mg GAE L^{-1}) with higher prediction accuracy (R_p = 0.99). In another study, NIR and FT-IR were investigated and compared based on the quantification of TPC in grape juice. Results showed that both techniques had comparable performance to determine TPC with low prediction errors. However, FT-IR showed an RMSEP (0.21 mg GAE100 mL^{-1}) which was moderately better than that of NIR (0.37 mg GAE100 mL^{-1}) (Caramês et al. 2017b).

FT-IR (1660 variables) and Raman (2644 variables) were also compared for quantification of TPC in Chinese rice wine. The authors compared several preprocessing techniques based on prediction results (Wu et al. 2016). The optimal preprocessing technique for FT-IR was 1st derivative with Savitzky-Golay smoothing and Raman was Savitzky-Golay smoothing. In this article, the authors also compared Si-PLS and PLS models for prediction of TPC. It was observed that Si-PLS models for both techniques presented high predictions with R^2_p of 0.9237 for FT-IR and R^2_p of 0.9064 for Raman as compared to PLS model with R^2_p of 0.9064 for Raman and R^2_p of 0.8918 for FT-IR. The results of this article demonstrated that the accuracy of models based on the Raman data was superior to those based on the FT-IR data. FT-Raman of honey showed very high accuracies for TPC (R_p = 99.9, RMSEP = 1.44 mg 100^{-1}g) when PLS and preprocessing such as straight-line subtraction and MSC were employed (Anjos et al. 2018).

Recently, a multispectral technique coupled with BPNN modeling for quantitative analysis of carotenoid and TPC in tomato samples was investigated (Liu et al. 2015a). Results

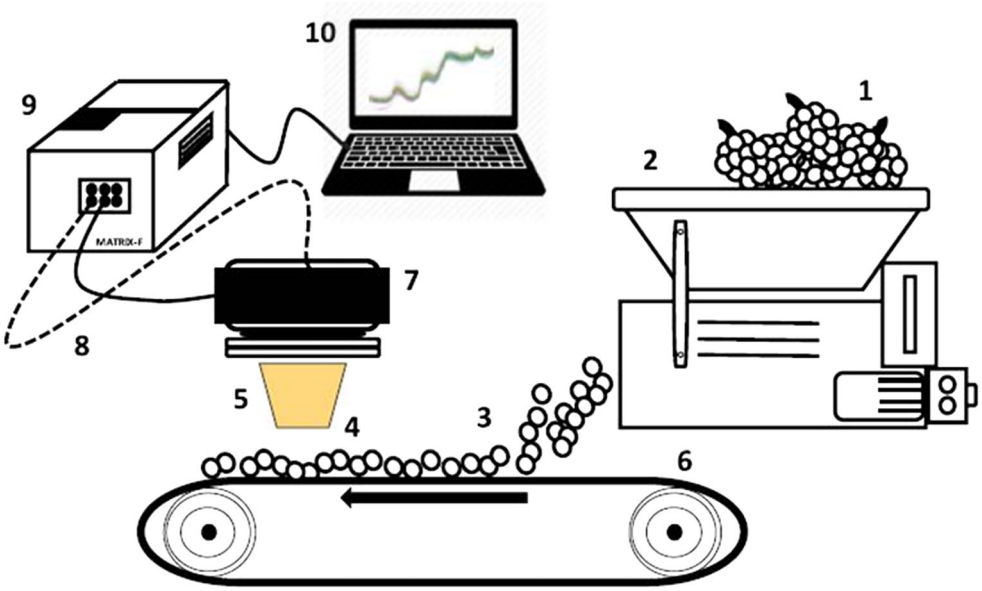

Fig. 5 Schematic illustration of the experimental setup for the spectral data collection using a conveyor belt moving online system (Aleixandre-Tudo, Nieuwoudt et al. 2019)

1: harvest; 2: crusher and destemmer; 3: intact or crushed berries; 4: the measuring diameter is approximately 10–12 cm; 5: light beam (17 cm measuring distance); 6: conveyor belt; 7: NIR light emission head; 8: fibre optic cable; 9: Matrix-F FT-NIR spectrometer; 10: spectral data collection.

demonstrated the feasibility of multispectral imaging application for accurate and rapid evaluation of bioactive compounds such as lycopene (R^2_p = 0.938, RMSEP = 2.29 mg kg^{-1}) and TPC (R^2_p = 0.965, RMSEP = 0.31 mg GAE 100 g^{-1}) distribution in tomato fruits.

Analysis of Total Flavonoids

NIR technique was evaluated toward the determination of TFC propolis, karkade tea, honey, apple, mint tea, and coffee. It was observed that PLSR was the most widespread method for measuring TFC in various foods. The popular models for detections of TFC were MPLS, PLS, and LS-SVM combined with a wide range of spectra, close to full-wavelength models. The correlation coefficients in raw propolis were R^2_p = 0.96 (Revilla et al. 2017), goji berry R_p = 0.9075 (Tingting et al. 2016), Karkade tea R_p = 0.83 (Tahir et al. 2016a, b, c), and honey R_p = 0.95 (Tahir et al. 2016a, b, c). Revilla et al. (2017) and Betances-Salcedo et al. (2017) successfully applied NIR equipped with remote reflectance fiber-optic probe to ground up propolis for determining the TFC raw propolis. The result showed that NIR technology with a fiber-optic probe could be used as an alternative to the chemical methods.

ATR-FT-IR was also evaluated for prediction of TFC in Moscatel dessert wines (Silva et al. 2014). PLS model on the fingerprint zones (1800–900 cm^{-1}) yielded higher prediction (R_p = 0.811) with a lower error of prediction (REP = 0.20%).

Analysis of Anthocyanins

NIR was also evaluated for determination of TAC in various foods. For measuring of TAC, Tahir and co-authors applied NIR together with PLS to predict the TAC in karkade tea (R_p = 0.91) (Tahir et al. 2016b). In similar research, Viegas et al. (2016) used NIR combined with PLS to quantify TAC in Wax Jambu fruit. The authors compared the performance of various pretreatments (such as smoothing, MSC, 1st Der, and 2nd Der). PLS combined with 2nd derivative showed the highest correlation (R_p = 0.98) and RPD (5.19) with the lowest prediction error (RMSEP = 9.0 mg L^{-1}). More recently, NIR was used to evaluate TAC in pomegranate (Arendse et al. 2017). In this study, two NIR acquisition approaches, i.e., integrating sphere (1064–1333, 1640–1835 nm) and emission head (1064–1333, 1640–1835 nm), were compared. Among the two NIR acquisition approaches, emission head (EH) showed the TAC (R^2_p = 70.50) with lower prediction error (RMSEP = 0.13 g GAE L^{-1}). NIR was applied to measure the TAC in flowering tea (i.e., *Camellia japonica*, *Hibiscus sabdariffa*, *Rosa chinensis*, *Rosa rugosa*, *Dianthus caryophyllus*, and *Myosotis sylvatica*) (Xiaowei et al. 2014). In this article, interval PLS (iPLS), a colony optimization interval partial least squares (ACO-iPLS), and genetic algorithm interval partial least squares (GA-iPLS) were applied on the data with superiority given to ACO-iPLS, as acquired in the characteristic regions for TAC (4590–4783, 5770–5963 cm^{-1}). Based on the selected region, ACO-iPLS yielded higher predictions (R_p = 0.9524) with lower prediction error

(RMSEP = 0.12 mg/g). Similarly, the possibility of application of NIR coupled with PLS algorithm to quantitatively determine the TAC in açaí (*Euterpe oleracea* Mart.) and *palmitero-juçara* (*Euterpe edulis* Mart.) fruits was investigated (Inácio et al. 2013). The *i*SPA-PLS model using smoothing preprocessing with a window of 5 points revealed better prediction than the model built with spectra pretreated by 1st Der combined with 2nd Der, demonstrating the effectiveness (R^2_p = 0.90, RMSEP = 9.35 g kg^{-1}) of the smoothing (with 5-point method) (Mariani et al. 2015). Based on NIR spectra together with the PLS model containing 600 variables, TAC in Jaboticaba fruit could be successfully quantified (R^2_p = 0.89). Other authors found that the NIR spectroscopy could be employed to determine TAC in black Goji berry accurately with Si-PLS model estimation (R_p = 0.899, RMSEP = 0.60 mg/g) (Yahui et al. 2017). PLS with 2nd Der presented higher prediction results (R^2_p = 0.86).

In another study, NIR (10,000–8450 cm^{-1}) and FT-MIR (747.42–829.11 cm^{-1}) were used for quantifying TAC in grape juice (Caramês et al. 2017b). In the case of the PLS model, both spectroscopies had a similar satisfactory performance to predict TAC presenting low RMSEP = 4.22 mg 100 g^{-1} for FT-MIR and RMSEP = 4.44 mg 100 g^{-1} for NIR. Additionally, the coefficient of determination was relatively equal to R^2_c = 0.81 for FT-MIR and R^2_c 0.84 for NIR.

FT-IR (4000–650 cm^{-1}) coupled with the PLS model was used to predict TAC in red and rose wine (Canan and Banu 2017). Several spectral preprocessing techniques were applied before the PLS model analysis of FT-IR spectra. In some FT-IR study, the cross-validation of the TAC model indicated a weak performance (Andrianjaka-Camps et al. 2015). This result could be attributed to the small number of raspberries puree used for developing PLS model. An analysis with a larger number of samples may be considered to enhance the performance of the model.

The potential of HSI technique to quantify TAC in foods has been studied. In this regard, the feasibility of HSI to measure TAC in wine grapes was reported (Chen et al. 2015). The prediction based on SVR with 60 latent values obtained from PLS with smoothed spectra had the highest prediction accuracy (R^2_p = 0.9414, RMSEP = 0.0046 mg g^{-1}) as compared to PLS model (R^2_p = 0.8407, RMSEP = 0.0129 mg g^{-1}). In another article, the feasibility of HSI for screening the nonacylated and total anthocyanins on the intact red grape during ripening was described (Hernández-Hierro et al. 2013). The MPLS models with fingerprint zones (950–1650 nm) demonstrated the potential of measuring both nonacylated (R^2_p = 0.86, SECV = 1.70 mg g^{-1}) and total anthocyanins (R^2_p = 0.86, SECV = 2.41 mg g^{-1}). However, the high correlation achieved between the compounds revealed that it is not possible to verify whether the results of HSI technique for measuring the composition nonacylated anthocyanins were attributable to their real absorbance or the relationship among nonacylated anthocyanins and total anthocyanins (Hernández-Hierro et al. 2013). Again, HSI was successfully employed for quantitative determination (R^2_p = 0.92) of TAC in lychee pericarp during storage of samples (Y.-C. Yang et al. 2015). Wavelength selection technique, such as successive projection algorithm (SPA) and stepwise regression (SWR), was applied to the spectral data. Based on selected wavelengths by SWR (11 bands) and SAP (9 bands), RBF-SVR model attained worse results for SPA-RBF-SVR (R^2_P = 0.672, RMSEP = 0.93 mg g^{-1}) and SWR-RBF-SVR (R^2_p = 0.712, RMSEP = 0.84 mg g^{-1}) as compared with RBF-SVR based on full-wavelength models (R^2_p = 0.916, RMSEP = 0.51 mg g^{-1}). This technique coupled with LS-SVM also was efficiently (R^2_p = 0.959, RMSE = 0.146 mg g^{-1}) employed for quantitative analysis of TAC in mulberry fruit (Huang et al. 2017). Similar performance (R^2_p = 0.866, RMSECV = 0.32 mg g^{-1}) was observed in the study conducted by Y. Liu et al. (2017). HSI technique was also successfully employed for the determination of TAC in wine grape with R^2_p of 0.907 (Gomes et al. 2017).

Analysis of Individual Phenolic Compounds

Non-destructive measurement of individual phenolic, flavonoid, and anthocyanin has also been developed and the evidence can be found in a number of the articles presented in this work (Table 2).

NIR spectroscopy combined with chemometric was applied to analyze nine individual catechin, total catechin, and gallic acid in green tea leaves. MPLS models presented high reproducibility and sensitivity for detection of catechins in the leaves of green tea, simultaneously improving its rapid and cost-effective features (Lee et al. 2014). Cross-validation models showed good correlations (R^2_p = 0.58–0.97) between reference measurements and NIR estimates. Inarejos-García et al. (2013) investigated the use of NIR (12,500–4000 cm^{-1}) combined with chemometric for the determination of several phenolic compounds in olive oil. Although most of the compounds showed satisfactory results, hydroxytyrosol and tyrosols showed very low correlations, indicating that the NIR technique could not be used for the quantitative analysis of these minor compounds in olive oil (Table 2). The application of NIR techniques combined with chemometrics for assessing individual phenolic acid and flavonoid in food was comprehensively demonstrated (Table 2). A comparison between the capability of NIR and HPLC methods suggested an overall agreement between these two methodologies. However, NIR has some advantages compared to HPLC. For example, NIR is cost-effective and time-saving, and it enables a substantial reduction in chemicals with minimal sample preparation. Aleixandre-Tudo et al. (2018) employed FT-NIR, FT-MIR, and FT-IR to monitor the main individual phenolic compounds during wine fermentation. FT-NIR

appeared to be the most accurate procedure to predict the phenolic content. Although slightly less accurate models were established, ATR-MIR and FT-IR can also be applied for the prediction of the majority of phenolic compounds. While the abovementioned publications demonstrated the potential of NIR for measurement of specific bioactive compounds, some authors recommended that its reliability needs to be further modernized, expanded, and enhanced with more samples (Ferrer-Gallego et al. 2011; Lee et al. 2014). Generally, FT-NIR appears to be the most accurate to quantify the phenolic compounds as compared with the other techniques.

FT-IR was employed for the prediction of various phenolic acid in coffee beans (Table 2). Results provided evidence of excellent performance for measurement of nine phenolic compounds ($R^2_p < 0.92$) for various chlorogenic acid isomers in coffee beans (Liang et al. 2016). In this article, for the first time, FT-IR was applied to the pure standard of chlorogenic acid isomers in order to extract the fingerprint regions (1700–1500, 1300–800 cm^{-1}) to build PLS models and quantify individual chlorogenic acid isomer concentration in coffee beans. FT-IR also was employed for screening the main proanthocyanidins in chocolate (Hu et al. 2016). Chocolates and the (+)-catechin standard were analyzed in the range of 4000–550 cm^{-1} and fingerprinting region (1800–700 cm^{-1}) was selected based on the targeted functional groups that appeared in (+)-catechin region. The obtained PLS results ($R^2_p <$ 0.72) recommended the possible use of FT-IR for applications in the food industry and commercial laboratories. Another FT-IR application was established to predict individual anthocyanin in red grape must (Rasines-Perea et al. 2015). However, the results showed the unsuitability of this technique for its application in red grape musts (R^2_p = 0.46–00.66). Some FT-IR investigations showed worse results and some components were not detected (for example, vanillic, cinnamic, caffeic, and p-coumaric acids) when used for quantification of low-concentration compounds (Uncu and Ozen 2015). A comparative analysis was carried out in order to validate the performance of FT-IR and Raman techniques, as well as their combination, in the determination of individual phenolic compounds in honey. Generally, FT-IR and Raman methodologies presented good results ($R^2_p < 0.99$) (Tahir et al. 2017). In this study, only samples of Sudanese honey varieties were presented for examination. Therefore, a further study involving large samples from different countries is needed before such methods can be adopted by food, pharmaceutical, and apiculture industries with confidence. Several anthocyanin concentrations of wine that were analyzed by MIR spectroscopy showed acceptable prediction results (R^2_{val} = 0.38–0.81), suggesting that this technique could be used to screen the changes of these compounds at different stages of the production process and mainly aging (Sen et al. 2016). BP-ANN models showed high performance (R^2_p = 0.9679), and the average relative error was 0.80%, which revealed the accuracy of the projected method and provided a theoretical basis for the applications of HSI in non-destructive determination for interior quality of soybean (Kezhu et al. 2014).

Analysis of Vitamins

Many studies have focused on the analysis of raw materials to investigate their potential antioxidant activity over the past three decades. However, in most of these studies, chlorophyll had not been involved in the trials regardless of the fact that it is the major pigment in nature (Lanfer-Marquez et al. 2005). Blanco-Díaz et al. (2014) employed NIR combined with MLS model to predict the chlorophylls in summer squash and reached good prediction results (R^2_p), where chlorophyll-a was 0.66 and chlorophyll-b was 0.79. Furthermore, the feasibility of NIR technique to quantify lycopene in carrot was studied (Ding et al. 2016). The results indicated better performance (R_p = 0.939), when radial basis function neural networks (RBF-NN) was applied to the NIR data. Nordey et al. (2014) also conducted a feasibility study on the application of portable NIR spectroscopy (350 to 2500 nm) coupled with PLS model to measure various bioactive components (i.e., chlorophyll-a, chlorophyll-b, carotenoid) in mango peel surface. The PLS models appeared to be very promising, particularly the ones achieved for the measurement of chlorophyll-a and chlorophyll-b (R^2_p = 0.99). NIR data of summer squash fruit flesh and skin were used to predict individual and total carotenoids (Martínez-Valdivieso et al. 2014). This result showed that NIR had good potential for the high-performance monitoring of total carotenoids (R^2_p = 0.95) and in specific components such as lutein (R^2_p = 0.96) and β-carotene (R^2_p = 0.81), indicating that NIR is a promising tool for the non-destructive determination of carotenoid profiles. Also, the NIR technique with PLS modeling was used for the prediction of carotenoid in honey and the results were very promising (R_p = 0.96) (Tahir et al. 2016b). Furthermore, the NIR technique was applied for the prediction of individual carotenoid in tomato juice. Results revealed the satisfactory performance of the projected method ($R^2_{cv} < 0.75$), for the analysis of cis-lycopene diepoxide, lycoxanthin, zeaxanthin, and β-carotene in tomato juice sample (Deak et al. 2015). NIR technique was also used to quantify β-carotene in mango fruit and high accuracy (R^2_p = 0.84, SECV = 16.55 retinol equivalents 100 g^{-1}) was achieved based on the MLR model (Rungpichayapichet et al. 2015).

Tocopherol such as α-tocopherol, β-tocopherol, δ-tocopherol, and γ-tocopherol and γ-tocotrienol is a form of vitamin E and natural antioxidant with regulatory cellular and molecular roles (Kim and Cho 2015; Žilić et al. 2016). NIR technique was also successfully (R^2_p = 0.865) used for the determination of vitamin E in quinoa (Moncada et al. 2013). NIR spectroscopy showed a high potential to analyze several tocopherols in olive oil (Cayuela and García 2017). These

authors compared the prediction results attained by NIR and Vis-NIR range. Results achieved by the two acquisitions were promising, particularly for α-tocopherol, γ-tocopherol, and total tocopherols (R_p = 0.91) while β-tocopherol showed the worse result (R_p = 0.41). Similarly, Inarejos-García et al. (2013) showed that FT-NIR had lower (R = 0.14) prediction results of β-tocopherol in olive oil.

Vitamin C (L-ascorbic acid) is an essential water-soluble antioxidant originating from citrus and other fruits. It may be a factor in cardiovascular, immune cell development, and iron use function in human (Gallie 2013). Vibrational spectroscopies were previously used for prediction of water-soluble vitamins (Blanco et al. 1993; Wojciechowski et al. 1998; H. Yang and Irudayaraj 2002). However, most of these studies were performed in pharmaceutical products. Most recently, NIR seems to be a promising technique for quantification of ascorbic acid in foods. In many studies, the simple PLS and MPLS models were feasible in the quantification of ascorbic acid in cashew apple, guava nectar, and guava pulp using NIR spectroscopy, producing high prediction (R^2_p about 0.85 for guava products and 0.84 for cashew fruit) (Alamar et al. 2016; Caramês et al. 2017a). According to Andrianjaka-Camps et al. (2015), the least square support vector machine (LS-SVM) showed the feasibility of quantifying ascorbic acid in apple using NIR spectroscopy. The results of the LS-SVM model presented an accurate estimation of ascorbic acid in apple (R^2_p = 0.80). A similar result of LS-SVM (R_p = 0.83) was observed when NIR was used for the prediction of ascorbic in orange samples (Liu et al. 2015b). Additionally, this technique was applied in the determination of ascorbic acid in summer squash with R^2_p of 0.86 (Blanco-Díaz et al. 2014) and passion fruit with R_p of 0.663 (Maniwara et al. 2014). The authors attributed the lower calibration and prediction results to the low concentration of ascorbic acid content and physical characteristics of passion fruits such as a waxy pericarp and thick mesocarp. A similar result (R^2_p = 0.61) was observed in cabbage (Kramchote et al. 2014); this result was expected since the ascorbic acid is not the main compound in cabbage. Beghi et al. (2013) also investigated ascorbic acid in Stark Red Delicious and Golden Delicious apple samples by portable NIR technique (450–980 nm) combined with PLS. However, the results revealed that NIR spectroscopy was not effective for evaluation of ascorbic acid in apples. The lower prediction results (R^2_{cv} = 0.40) in Stark Red Delicious could be justified by a very low concentration of this component in this cultivar. FT-NIR, FT-MIR, and FT-IR were used comparatively for prediction of ascorbic acid in pomegranate juice (Arendse et al. 2018). The result of FT-NIR technique was very promising for quantifying ascorbic acid (R^2_p = 0.709). Similar findings were achieved from the application of NIR by integrating sphere as an acquisition method, which enabled the prediction of ascorbic acid in pomegranate with high accuracy as presented in Table 2. Quantification of ascorbic acid concentration in raspberry puree using FT-IR was conducted by Andrianjaka-Camps et al. (2015), who found that Si-PLS model was far more accurate (R^2_p = 0.94) in the determination of ascorbic than those reported using NIR spectroscopy. A comparative study was conducted in order to measure the feasibility of NIR and MIR techniques in the determination of carotenoids in passion fruit. Overall, NIR slightly showed high performance (R^2_{cv} = 0.56, RMSECV = 0.04 mg g^{-1}) than MIR spectroscopy (R^2_{cv} = 0.772, RMSECV = 0.045. However, both techniques presented low prediction results and the authors attributed that to the low concentration of carotenoid in passion fruit (G. A. de Oliveira et al. 2014).

Carotenoid is considered to be an effective bioactive component and may have protected cells against oxidative damage and, potentially, reduce the risk of cancer particularly prostate cancer (Martí et al. 2016). Indeed, lycopene is the main carotenoid determined in tomatoes, constituting about 80–90% of the total pigment contents (Rizk et al. 2014). In the case of Raman spectroscopy, different Raman zones (i.e., 200–2000, 300–1900, 900–1650, 1100–1600 cm^{-1}) with PLS were used to quantify lycopene in tomato fruits (Fu et al. 2016). However, all PLS models failed to quantify lycopene content accurately with the lower prediction (R_p = 0.57) and high prediction error (SEP = 14.2 μg g^{-1}). The authors, therefore, attributed the poor results to heterogeneous samples and poor laser power (Fu et al. 2016). In another study, Krähmer et al. (2016) compared the effect of various pretreatment methods on the different FT-Raman spectral range to quantify individual and total carotenoids in carrots with high predictions (R^2_p < 0.80). Similar prediction result (R^2_p about 0.85) was observed from the application of Raman for determination of total carotenoid in the carrot (Lawaetz et al. 2016). Recently, Raman spectroscopy together with PLS model for carotenoid determination in processed sweet potato was studied (Sebben et al. 2018). The prediction results for the sample treated with hot air was R^2_p = 0.90 and by microwave was R^2_p = 0.88. Although Raman technique showed great potential for quantitative analysis of this compound, satisfactory reproducibility of Raman predictions relies on the features of the sample and its condition after processing. For instances, sample dried using microwave showed higher prediction, although RMSEC of these groups was higher than samples of hot air samples. From the abovementioned studies, food and pharmaceutical industries can practically make use of these vibrational spectroscopies which are not laborious but cost-efficient in the analysis of vitamins.

Analysis of Volatile Compounds

Good functional food must provide both nutrient-specific health-promoting functionality and satisfactory sensory characteristic to meet consumer requirements (Sun-Waterhouse and Wadhwa 2013). Recently, the NIR technique was

investigated for the determination of the aroma compounds in white wines during different stages of storage (Genisheva et al. 2018). For extraction of the useful information, PCA was applied and PLS models were used for the quantification of the volatile compounds. The derived models using NIR data and PLS presented high predictions ($R^2_p \leq 0.95$) and can be used for other types of wine or even to the entire food field. Musty taint odor is unpleasant organoleptic defects in wines and it is a serious problem in winemaking worldwide (Apostolou et al. 2014). In this regard, the NIR technique was used to screen haloanisoles and halophenols accountable for musty taint defect in barrel aged red wines. From the results, the prediction of haloanisoles and halophenols using GC-MS and NIR together with PLS model was good (R^2_p about 0.80). The authors concluded that these compounds can be monitored rapidly and simply by this technique (Garde-Cerdán et al. 2012). However, the prediction errors achieved were below the sensory threshold standards described for these compounds, making this method unsuitable (dos Santos et al. 2017). The major aroma compounds of lavandin and lavender oils were investigated using NIR spectroscopy (Table 3). Apparently, the correlation coefficients (R^2_p = 0.97) obtained from the PLS regression were satisfactory (Lafhal et al. 2016). In addition, the results indicated that this technique might be applied to other oils commonly used in medicine and other fields. Furthermore, NIR was used for the determination of low concentrations of aroma compounds in olive oil (Inarejos-García et al. 2013). However, poor correlations were observed for some components such as E-2-hexenal (R_p = 0.42) and C6 aldehydes (R_p = 0.43).

NIR with remote fiber-optic reflectance probe to analyze volatile compounds in cheeses (González-Martín et al. 2014). The calibration models developed using 67–72 samples of cheese had a correlation coefficient (R^2) between 0.600 for the 3-methyl-1-butanol and 0.903 for the 2-nonanone. In this study, the robustness of the MPLS models was confirmed by applying it to 20 new samples of different compositions and ripening times, which did not belong to the calibration set. The results of that study showed that NIR was similar to those of the purge-and-trap gas chromatography-mass spectrometry (Table 3). Measurement of aromatic plant terpenoid content is an important issue in many aspects. Results from Ercioglu et al. (2018) summarized in Table 3 showed that NIR can be used to predict terpenoid profile in plants with high coefficient of determination (R^2) values in the range of 0.953–0.997. These results demonstrated that NIR could provide worthy information with respect to aromatic plant authentication, impurity, and chemotypes in consideration of a variety of terpenoid compounds. Spectroscopic investigations have been established for FT-NIR to monitor the off-flavors in olive oil (Inarejos-García et al. 2013). The results showed that FT-NIR is a powerful technique that allows rapid monitoring of cornicabra virgin olive oil samples to determine their volatile profile and thus their quality and commercial grade. The volatile compounds were well correlated with the FT-NIR spectra in the case of C6 alcohols (r = 0.69–0.80), accountable for the green sensory notes in high-quality cornicabra virgin olive oils. Although the FT-NIR showed promising results, further research is required by sampling various varieties of olive oils from different geographical areas before applying FT-NIR for screening the flavor of olive oils in the food industry. A similar trend was found when the NIR technique was used to monitor the alcohol strength during fermentation of apple wine (Peng et al. 2016).

Most recently, a comparative study was conducted in order to assess the potential of using NIR, MIR, and Raman techniques for determination of alcoholic strength in wine (Teixeira dos Santos et al. 2018). Overall, MIR technique revealed an excellent performance in the establishment of calibration models for the determination of alcoholic strength in white wine (Table 3).

FT-Raman was used to predict natural pesticides (e.g., antifungal) in carrot including falcarinol, falcarindiol, and 3-*O*-acetylfalcarindiol (Krähmer et al. 2016). The results showed that FT-Raman could be used for quantitative analysis of falcarindiol while falcarinol and 3-*O*-acetylfalcarindiol models can be used for screening purpose. Although the NIR and Raman showed great potential for prediction of volatile compounds in the oils, wine, cheese, and aromatic plant, future investigations are required to demonstrate the feasibility of their applications in industrial settings.

Technical Challenges and Future Trends

Advances in IR, Raman, and HSI techniques have presented enormous opportunities for the research community, pharmaceutical, and food industries to establish rapid, non-destructive analytical, and environmental-friendly methods for food bioactive materials and aroma inspection. Based on these no-preparation and chemical-free assessment methodologies, the analysis time can be reduced and the errors arising during the extraction of the bioactive active or aroma compounds can also be decreased. Concerning all of the environmentally friendly technologies reviewed and discussed in this article, there are still some issues that impede the adaptation of the latest scientific research achievement obtained in a laboratory level to industrial implementations. These include (a) requirement for specific mathematics knowledge to perform this task; (b) building appropriate preprocessing method to reduce the influence of physical impacts on raw spectral data; (c) establishing state-of-the-art spectral analysis procedures capable of filtering useless information; (d) manipulating proper chemometric approaches for enhancing the model accuracy for simultaneous implementations; and (e) reducing the price of the technologies. Then, the chemical properties of functional

groups of foods presented in the spectra will be used for quantitative analysis of biologically active materials and aroma compounds effectively. Thus, the food and nutraceutical industries can practically take advantage of the opportunity to implement these non-destructive approaches without laborious and inefficient chemical assays and thus prominently improve the monitoring quality and biologically active material in foods. A previous study (Aleixandre-Tudo et al. 2019) showed NIR had achieved success in measuring of phenolic compound in whole and crushed berries that are transported on a moving conveyor belt. Thus, future work should focus on enhancing the efficiency of previously presented algorithms, which may increase the prediction accuracy of the model. To some extent, the application of vibrational spectroscopies in volatile compounds analysis is still not at a mature stage and a limited number of studies have been published. Thus, further study is expected to establish useful algorithms existing in other fields for their applications in aromatic compound detection.

Conclusions

The recent publications in the field of vibrational spectroscopy indicated that NIR, FT-IR, and Raman could provide accurate measurement for bioactive and volatile compounds of various foods. Obviously, not only is the application of vibrational spectroscopy to analyze biological active materials and aromatic compounds limited to laboratory application but also, in some cases, online measurement has been reported. However, the frequencies of application of vibrational spectroscopies to determine biological active material and aroma profile were varied greatly. Figure 4 indicated the number of published articles on applying various vibrational spectroscopies for determinations of various bioactive and volatile compounds in food during the period of July 2011 to January 2019. It is obvious from this figure that NIR was more used for determination of bioactive compounds and volatile compounds followed by FT-IR techniques. Although Raman and HSI techniques were fewer applications in this field, an increasing number of research works in the past few years have demonstrated their application for measurement of bioactive compounds in food. This article shows that infrared spectroscopy, Raman, and HSI techniques are now convenient approaches to evaluate the maturity and antioxidants, and able to characterize raw and processed foods, and monitor products during storage and processing.

Funding Information This study received financial support from the National Natural Science Foundation of China (31750110458, 2017) and the China Postdoctoral Science Foundation (2017M611736, 2017).

Compliance with Ethical Standards

This article does not contain any studies with human or animal subjects.

Conflict of Interest Haroon Elrasheid Tahir declares that he has no conflict of interest. Zou Xiaobo declares that he has no conflict of interest. Xiao Jianbo declares that she has no conflict of interest. Shi Jiyong declares that he has no conflict of interest. Gustav Komla Mahunu declares that he has no conflict of interest. Jun-Li Xu declares that he has no conflict of interest. Da-Wen Sun declares that he has no conflict of interest.

Informed Consent Informed consent is not applicable in this study.

References

Alajtal AI (2010) Application for the analysis of organic compounds and minerals of astrobiological significance. The detection and discrimination of organic compounds and mineral analogues in pure and mixed samples of astrobiological significance using Raman spectroscopy, XRD and scanning electronmicroscopy. PhD Dissertation, University of Bradford. http://hdl.handle.net/10454/4425. Accessed 2 Jan 2019

Alamar PD, Caramês ETS, Poppi RJ, Pallone JAL (2016) Quality evaluation of frozen guava and yellow passion fruit pulps by NIR spectroscopy and chemometrics. Food Res Int 85:209–214. https://doi.org/10.1016/j.foodres.2016.04.027

Aleixandre-Tudo JL, Nieuwoudt H, Aleixandre JL, du Toit W (2018) Chemometric compositional analysis of phenolic compounds in fermenting samples and wines using different infrared spectroscopy techniques. Talanta 176:526–536. https://doi.org/10.1016/j.talanta.2017.08.065

Aleixandre-Tudo JL, Nieuwoudt H, du Toit W (2019) Towards on-line monitoring of phenolic content in red wine grapes: a feasibility study. Food Chem 270:322–331. https://doi.org/10.1016/j.foodchem.2018.07.118

Andrianjaka-Camps Z-N, Baumgartner D, Camps C, Guyer E, Arrigoni E, Carlen C (2015) Prediction of raspberries puree quality traits by Fourier transform infrared spectroscopy. LWT Food Sci Technol 63(2):1056–1062. https://doi.org/10.1016/j.lwt.2015.04.062

Anjos O, Santos AJA, Paixao V, Estevinho LM (2018) Physicochethical characterization of Lavandula spp. honey with FT-Raman spectroscopy. Talanta 178:43–48. https://doi.org/10.1016/j.talanta.2017.08.099

Apostolou T, Pascual N, Marco MP, Moschos A, Petropoulos A, Kaltsas G, Kintzios S (2014) Extraction-less, rapid assay for the direct detection of 2,4,6-trichloroanisole (TCA) in cork samples. Talanta 125:336–340. https://doi.org/10.1016/j.talanta.2014.03.023

Arendse E, Fawole OA, Magwaza LS, Nieuwoudt HH, Opara UL (2017) Development of calibration models for the evaluation of pomegranate aril quality by Fourier-transform near infrared spectroscopy combined with chemometrics. Biosyst Eng 159:22–32. https://doi.org/10.1016/j.biosystemseng.2017.04.004

Arendse E, Fawole OA, Magwaza LS, Nieuwoudt H, Opara UL (2018) Comparing the analytical performance of near and mid infrared spectrometers for evaluating pomegranate juice quality. LWT 91:180–190. https://doi.org/10.1016/j.lwt.2018.01.035

Ayseli MT, İpek Ayseli Y (2016) Flavors of the future: health benefits of flavor precursors and volatile compounds in plant foods. Trends Food Sci Technol 48:69–77. https://doi.org/10.1016/j.tifs.2015.11.005

Baeten V, Dardenne P (2002) Spectroscopy: developments in instrumentation and analysis. Grasas Aceites 53(1):45–63

Beghi R, Spinardi A, Bodria L, Mignani I, Guidetti R (2013) Apples nutraceutic properties evaluation through a visible and near-infrared portable system. Food Bioprocess Technol 6(9):2547–2554. https://doi.org/10.1007/s11947-012-0824-7

Betances-Salcedo E, Revilla I, Vivar-Quintana AM, Gonzalez-Martin MI (2017) Flavonoid and antioxidant capacity of propolis prediction using near infrared spectroscopy. Sensors (Basel) 17(7). https://doi.org/10.3390/s17071647

Bianchi F, Careri M, Musci M (2005) Volatile norisoprenoids as markers of botanical origin of Sardinian strawberry-tree (Arbutus unedo L.) honey: characterisation of aroma compounds by dynamic headspace extraction and gas chromatography–mass spectrometry. Food Chem 89(4):527–532. https://doi.org/10.1016/j.foodchem.2004.03.009

Blanco M, Coello J, Iturriaga H, Maspoch S, de la Pezuela C (1993) Determination of ascorbic acid in pharmaceutical preparations by near infrared reflectance spectroscopy. Talanta 40(11):1671–1676. https://doi.org/10.1016/0039-9140(93)80083-4

Blanco-Díaz MT, Del Río-Celestino M, Martínez-Valdivieso D, Font R (2014) Use of visible and near-infrared spectroscopy for predicting antioxidant compounds in summer squash (Cucurbita pepo ssp pepo). Food Chem 164:301–308. https://doi.org/10.1016/j.foodchem.2014.05.019

Boido E, Fariña L, Carrau F, Dellacassa E, Cozzolino D (2013) Characterization of glycosylated aroma compounds in tannat grapes and feasibility of the near infrared spectroscopy application for their prediction. Food Anal Methods 6(1):100–111. https://doi.org/10.1007/s12161-012-9423-5

Bumbrah GS, Sharma RM (2016) Raman spectroscopy – basic principle, instrumentation and selected applications for the characterization of drugs of abuse. Egypt J Forensic Sci 6(3):209–215. https://doi.org/10.1016/j.ejfs.2015.06.001

Bureau S, Cozzolino D, Clark CJ (2019) Contributions of Fourier-transform mid infrared (FT-MIR) spectroscopy to the study of fruit and vegetables: a review. Postharvest Biol Technol 148:1–14. https://doi.org/10.1016/j.postharvbio.2018.10.003

Burns DA, Ciurczak EW (2001) Handbook of near-infrared analysis, 3rd edn. CRC press. pp. 25-38

Canan C, Banu O (2017) Monitoring of wine process and prediction of its parameters with mid-infrared spectroscopy. J Food Process Eng 40(1):e12280. https://doi.org/10.1111/jfpe.12280

Caporaso N, Whitworth MB, Fowler MS, Fisk ID (2018) Hyperspectral imaging for non-destructive prediction of fermentation index, polyphenol content and antioxidant activity in single cocoa beans. Food Chem 258:343–351. https://doi.org/10.1016/j.foodchem.2018.03.039

Caramês ETS, Alamar PD, Poppi RJ, Pallone JAL (2017a) Quality control of cashew apple and guava nectar by near infrared spectroscopy. J Food Compos Anal 56:41–46. https://doi.org/10.1016/j.jfca.2016.12.002

Caramês ETS, Alamar PD, Poppi RJ, Pallone JAL (2017b) Rapid assessment of total phenolic and anthocyanin contents in grape juice using infrared spectroscopy and multivariate calibration. Food Anal Methods 10(5):1609–1615. https://doi.org/10.1007/s12161-016-0721-1

Cayuela JA, García JF (2017) Sorting olive oil based on alpha-tocopherol and total tocopherol content using near-infra-red spectroscopy (NIRS) analysis. J Food Eng 202:79–88. https://doi.org/10.1016/j.jfoodeng.2017.01.015

Chen S, Zhang F, Ning J, Liu X, Zhang Z, Yang S (2015) Predicting the anthocyanin content of wine grapes by NIR hyperspectral imaging. Food Chem 172:788–793. https://doi.org/10.1016/j.foodchem.2014.09.119

Cheng J-H, Nicolai B, Sun D-W (2017) Hyperspectral imaging with multivariate analysis for technological parameters prediction and classification of muscle foods: a review. Meat Sci 123:182–191. https://doi.org/10.1016/j.meatsci.2016.09.017

Cigic IK, Prosen H (2009) An overview of conventional and emerging analytical methods for the determination of mycotoxins. Int J Mol Sci 10(1):62–115. https://doi.org/10.3390/ijms10010062

Coates J (2000) Interpretation of infrared spectra, a practical approach. Encycl Anal Chem 12:10815–10837

D'Amico P, Armani A, Gianfaldoni D, Guidi A (2016) New provisions for the labelling of fishery and aquaculture products: difficulties in the implementation of Regulation (EU) n. 1379/2013. Mar Policy 71:147–156. https://doi.org/10.1016/j.marpol.2016.05.026

da Silva C, Prasniewski A, Calegari MA, de Lima VA, Oldoni TLC (2018) Determination of total phenolic compounds and antioxidant activity of ethanolic extracts of propolis using ATR–FT-IR spectroscopy and chemometrics. Food Anal Methods 11:2013–2021. https://doi.org/10.1007/s12161-018-1161-x

de Oliveira GA, de Castilhos F, Renard CM-GC, Bureau S (2014) Comparison of NIR and MIR spectroscopic methods for determination of individual sugars, organic acids and carotenoids in passion fruit. Food Res Int 60:154–162. https://doi.org/10.1016/j.foodres.2013.10.051

de Oliveira IRN, Roque JV, Maia MP, Stringheta PC, Teófilo RF (2018) New strategy for determination of anthocyanins, polyphenols and antioxidant capacity of Brassica oleracea liquid extract using infrared spectroscopies and multivariate regression. Spectrochim Acta A Mol Biomol Spectrosc 194:172–180. https://doi.org/10.1016/j.saa.2018.01.006

de Toledo TA, da Silva LE, Botelho TC, Ramos RJ, de Souza Jr PT, Teixeira AMR, Freire PTC, Bento RRF (2012) Characterization of flavonoid 3-methoxyquercetin performed by FT-IR and FT-Raman spectroscopies and DFT calculations. J Mol Struct 1029:22–27. https://doi.org/10.1016/j.molstruc.2012.06.058

Deak K, Szigedi T, Pek Z, Baranowski P, Helyes L (2015) Carotenoid determination in tomato juice using near infrared spectroscopy. Int Agrophys 29(3):275–282. https://doi.org/10.1515/intag-2015-0032

Ding X, Guo Y, Ni Y, Kokot S (2016) A novel NIR spectroscopic method for rapid analyses of lycopene, total acid, sugar, phenols and antioxidant activity in dehydrated tomato samples. Vib Spectrosc 82:1–9. https://doi.org/10.1016/j.vibspec.2015.10.004

Dong W, Ni Y, Kokot S (2013) A near-infrared reflectance spectroscopy method for direct analysis of several chemical components and properties of fruit, for example, Chinese Hawthorn. J Agric Food Chem 61(3):540–546. https://doi.org/10.1021/jf305272s

Dong W, Ni Y, Kokot S (2014) A novel near-infrared spectroscopy and chemometrics method for rapid analysis of several chemical components and antioxidant activity of mint (Mentha haplocalyx Brig.) samples. Appl Spectrosc 68(2):245–254. https://doi.org/10.1366/13-07091

dos Santos CAT, Páscoa RNMJ, Lopes JA (2017) A review on the application of vibrational spectroscopy in the wine industry: from soil to bottle. TrAC Trends Anal Chem 88:100–118. https://doi.org/10.1016/j.trac.2016.12.012

Dutta A (2017) Chapter 4 - Fourier transform infrared spectroscopy. In Thomas S, Thomas R, Zachariah AK, Mishra RK (Eds) Spectroscopic methods for nanomaterials characterization. Elsevier, pp. 73-93.

Erasmus RM, Comins JD (2018) Raman scattering. In: Ida N, Meyendorf N (eds) Handbook of Advanced Non-Destructive Evaluation. Springer International Publishing, Cham, pp 1–54

Eravuchira PJ, El-Abassy RM, Deshpande S, Matei MF, Mishra S, Tandon P, … Materny A (2012) Raman spectroscopic characterization of different regioisomers of monoacyl and diacyl chlorogenic acid. Vib Spectrosc 61:10-16. doi:https://doi.org/10.1016/j.vibspec.2012.02.009

Ercioglu E, Velioglu HM, Boyaci IH (2018) Determination of terpenoid contents of aromatic plants using NIRS. Talanta 178:716–721. https://doi.org/10.1016/j.talanta.2017.10.017

Fernández Pierna, J. A., Manley, M., Dardenne, P., Downey, G., & Baeten, V. (2018). Spectroscopic Technique: Fourier Transform (FT) Near-Infrared Spectroscopy (NIR) and Microscopy (NIRM). 2and edn. Academic Press, pp. 103-138.

Ferrer-Gallego R, Hernández-Hierro JM, Rivas-Gonzalo JC, Escribano-Bailón MT (2011) Determination of phenolic compounds of grape skins during ripening by NIR spectroscopy. LWT Food Sci Technol 44(4):847–853. https://doi.org/10.1016/j.lwt.2010.12.001

Frizon CNT, Oliveira GA, Perussello CA, Peralta-Zamora PG, Camlofski AMO, Rossa ÜB, Hoffmann-Ribani R (2015) Determination of total phenolic compounds in yerba mate (Ilex paraguariensis) combining near infrared spectroscopy (NIR) and multivariate analysis. LWT Food Sci Technol 60(2, Part 1):795–801. https://doi.org/10.1016/j.lwt.2014.10.030

Fu X, He X, Xu H, Ying Y (2016) Nondestructive and rapid assessment of intact tomato freshness and lycopene content based on a miniaturized raman spectroscopic system and colorimetry. Food Anal Methods 9(9):2501–2508. https://doi.org/10.1007/s12161-016-0440-7

Gallie DR (2013) Increasing vitamin C content in plant foods to improve their nutritional value—successes and challenges. Nutrients 5(9): 3424–3446. https://doi.org/10.3390/nu5093424

Gao F, Xu L, Zhang Y, Yang Z, Han L, Liu X (2018) Analytical Raman spectroscopic study for discriminant analysis of different animal-derived feedstuff: Understanding the high correlation between Raman spectroscopy and lipid characteristics. Food Chem 240: 989–996. https://doi.org/10.1016/j.foodchem.2017.07.143

Garde-Cerdán T, Lorenzo C, Zalacain A, Alonso GL, Salinas MR (2012) Using near infrared spectroscopy to determine haloanisoles and halophenols in barrel aged red wines. LWT Food Sci Technol 46(2):401–405. https://doi.org/10.1016/j.lwt.2011.12.012

Genisheva Z, Quintelas C, Mesquita DP, Ferreira EC, Oliveira JM, Amaral AL (2018) New PLS analysis approach to wine volatile compounds characterization by near infrared spectroscopy (NIR). Food Chem 246:172–178. https://doi.org/10.1016/j.foodchem.2017.11.015

Giovanelli G, Sinelli N, Beghi R, Guidetti R, Casiraghi E (2014) NIR spectroscopy for the optimization of postharvest apple management. Postharvest Biol Technol 87:13–20. https://doi.org/10.1016/j.postharvbio.2013.07.041

Gomes V, Fernandes A, Martins-Lopes P, Pereira L, Mendes Faia A, Melo-Pinto P (2017) Characterization of neural network generalization in the determination of pH and anthocyanin content of wine grape in new vintages and varieties. Food Chem 218:40–46. https://doi.org/10.1016/j.foodchem.2016.09.024

González-Martín I, Hernández-Hierro JM, González-Pérez C, Revilla I, Vivar-Quintana A, Lobos Ortega I (2014) Potential of near infrared spectroscopy for the analysis of volatile components in cheeses. LWT Food Sci Technol 55(2):666–673. https://doi.org/10.1016/j.lwt.2013.10.008

Hernández-Hierro JM, Nogales-Bueno J, Rodríguez-Pulido FJ, Heredia FJ (2013) Feasibility study on the use of near-infrared hyperspectral imaging for the screening of anthocyanins in intact grapes during ripening. J Agric Food Chem 61(41):9804–9809. https://doi.org/10.1021/jf4021637

Hu Y, Pan ZJ, Liao W, Li J, Gruget P, Kitts DD, Lu X (2016) Determination of antioxidant capacity and phenolic content of chocolate by attenuated total reflectance-Fourier transformed-infrared spectroscopy. Food Chem 202:254–261. https://doi.org/10.1016/j.foodchem.2016.01.130

Huang L, Zhou Y, Meng L, Wu D, He Y (2017) Comparison of different CCD detectors and chemometrics for predicting total anthocyanin content and antioxidant activity of mulberry fruit using visible and near infrared hyperspectral imaging technique. Food Chem 224:1–10. https://doi.org/10.1016/j.foodchem.2016.12.037

Inácio MRC, de Lima KMG, Lopes VG, Pessoa JDC, de Almeida Teixeira GH (2013) Total anthocyanin content determination in intact açaí (Euterpe oleracea Mart.) and palmitero-juçara (Euterpe edulis Mart.) fruit using near infrared spectroscopy (NIR) and multivariate calibration. Food Chem 136(3):1160–1164. https://doi.org/10.1016/j.foodchem.2012.09.046

Inarejos-García AM, Gómez-Alonso S, Fregapane G, Salvador MD (2013) Evaluation of minor components, sensory characteristics and quality of virgin olive oil by near infrared (NIR) spectroscopy. Food Res Int 50(1):250–258. https://doi.org/10.1016/j.foodres.2012.10.029

Jha, S. N. (2010). Near Infrared Spectroscopy. In S. N. Jha (Ed.), Nondestructive Evaluation of Food Quality: Theory and Practice, Berlin, Heidelberg: Springer Berlin Heidelberg, pp. 141-212.

Kadiroğlu P, Aydemir LY, Akcakaya FG (2018) Prediction of functional properties of registered chickpea samples using FT-IR spectroscopy and chemometrics. LWT 93:463–469. https://doi.org/10.1016/j.lwt.2018.03.080

Karoui, R. (2018). Spectroscopic Technique: Mid-Infrared (MIR) and Fourier Transform Mid-Infrared (FT-MIR) Spectroscopies. 2and edn. Academic Press, pp. 23-50

Kezhu T, Yuhua C, Weixian S, Xiaoda C (2014) Detection of isoflavones content in soybean based on Hyperspectral Imaging Technology. Sens Transducers 169(4):55

Khulal U, Zhao J, Hu W, Chen Q (2016) Nondestructive quantifying total volatile basic nitrogen (TVB-N) content in chicken using hyperspectral imaging (HSI) technique combined with different data dimension reduction algorithms. Food Chem 197:1191–1199. https://doi.org/10.1016/j.foodchem.2015.11.084

Kim Y-N, Cho Y-O (2015) Vitamin E status of 20-to 59-year-old adults living in the Seoul metropolitan area of South Korea. Nutr Res Pract 9(2):192–198. https://doi.org/10.4162/nrp.2015.9.2.192

Kizil, R., & Irudayaraj, J. (2018). Spectroscopic Technique: Fourier Transform Raman (FT-Raman) Spectroscopy. 2and edn. Academic Press, pp. 193-217

Krähmer A, Böttcher C, Rode A, Nothnagel T, Schulz H (2016) Quantifying biochemical quality parameters in carrots (Daucus carota L.) – FT-Raman spectroscopy as efficient tool for rapid metabolite profiling. Food Chem 212:495–502. https://doi.org/10.1016/j.foodchem.2016.05.176

Kramchote S, Nakano K, Kanlayanarat S, Ohashi S, Takizawa K, Bai G (2014) Rapid determination of cabbage quality using visible and near-infrared spectroscopy. LWT Food Sci Technol 59(2, Part 1): 695–700. https://doi.org/10.1016/j.lwt.2014.07.009

Lafhal S, Vanloot P, Bombarda I, Kister J, Dupuy N (2016) Chemometric analysis of French lavender and lavandin essential oils by near infrared spectroscopy. Ind Crop Prod 80:156–164. https://doi.org/10.1016/j.indcrop.2015.11.017

Lanfer-Marquez UM, Barros RMC, Sinnecker P (2005) Antioxidant activity of chlorophylls and their derivatives. Food Res Int 38(8):885–891. https://doi.org/10.1016/j.foodres.2005.02.012

Lawaetz AJ, Christensen SMU, Clausen SK, Jørnsgaard B, Rasmussen SK, Andersen SB, Rinnan Å (2016) Fast, cross cultivar determination of total carotenoids in intact carrot tissue by Raman spectroscopy and partial least squares calibration. Food Chem 204:7–13. https://doi.org/10.1016/j.foodchem.2016.02.107

Lee M-S, Hwang Y-S, Lee J, Choung M-G (2014) The characterization of caffeine and nine individual catechins in the leaves of green tea (Camellia sinensis L.) by near-infrared reflectance spectroscopy. Food Chem 158:351–357. https://doi.org/10.1016/j.foodchem.2014.02.127

Li Y-S, Church JS (2014) Raman spectroscopy in the analysis of food and pharmaceutical nanomaterials. J Food Drug Anal 22(1):29–48. https://doi.org/10.1016/j.jfda.2014.01.003

Li X, Jin J, Sun C, Ye D, Liu Y (2019) Simultaneous determination of six main types of lipid-soluble pigments in green tea by visible and

near-infrared spectroscopy. Food Chem 270:236–242. https://doi.org/10.1016/j.foodchem.2018.07.039

Liang N, Lu X, Hu Y, Kitts DD (2016) Application of attenuated total reflectance–Fourier transformed infrared (ATR-FTIR) spectroscopy to determine the chlorogenic acid isomer profile and antioxidant capacity of coffee beans. J Agric Food Chem 64(3):681–689. https://doi.org/10.1021/acs.jafc.5b05682

Liu C, Liu W, Chen W, Yang J, Zheng L (2015a) Feasibility in multi-spectral imaging for predicting the content of bioactive compounds in intact tomato fruit. Food Chem 173:482–488. https://doi.org/10.1016/j.foodchem.2014.10.052

Liu C, Yang SX, Deng L (2015b) Determination of internal qualities of Newhall navel oranges based on NIR spectroscopy using machine learning. J Food Eng 161:16–23. https://doi.org/10.1016/j.jfoodeng.2015.03.022

Liu Y, Sun Y, Xie A, Yu H, Yin Y, Li X, Duan X (2017) Potential of hyperspectral imaging for rapid prediction of anthocyanin content of purple-fleshed sweet potato slices during drying process. Food Anal Methods 10(12):3836–3846. https://doi.org/10.1007/s12161-017-0950-y

Ma L, Zhang Z, Zhao X, Zhang S, Lu H (2016) The rapid determination of total polyphenols content and antioxidant activity in Dendrobium officinale using near-infrared spectroscopy. Anal Methods 8(23):4584–4589. https://doi.org/10.1039/C6AY00542J

Magalhães LM, Machado S, Segundo MA, Lopes JA, Páscoa RNMJ (2016) Rapid assessment of bioactive phenolics and methylxanthines in spent coffee grounds by FT-NIR spectroscopy. Talanta 147:460–467. https://doi.org/10.1016/j.talanta.2015.10.022

Maniwara P, Nakano K, Boonyakiat D, Ohashi S, Hiroi M, Tohyama T (2014) The use of visible and near infrared spectroscopy for evaluating passion fruit postharvest quality. J Food Eng 143:33–43. https://doi.org/10.1016/j.jfoodeng.2014.06.028

Mariani NCT, de Almeida Teixeira GH, de Lima KMG, Morgenstern TB, Nardini V, Júnior LCC (2015) NIRS and iSPA-PLS for predicting total anthocyanin content in jaboticaba fruit. Food Chem 174:643–648. https://doi.org/10.1016/j.foodchem.2014.11.008

Marrassini C, Idrissi A, De Waele I, Smail K, Tchouar N, Moreau M, Mezzetti A (2015) Organic solvent–luteolin interactions studied by FT-Raman, Vis-Raman, UV-Raman spectroscopy and DFT calculations. J Mol Liq 205:2–8. https://doi.org/10.1016/j.molliq.2014.08.014

Martelo-Vidal MJ, Vázquez M (2014) Determination of polyphenolic compounds of red wines by UV–VIS–NIR spectroscopy and chemometrics tools. Food Chem 158:28–34. https://doi.org/10.1016/j.foodchem.2014.02.080

Martí R, Roselló S, Cebolla-Cornejo J (2016) Tomato as a source of carotenoids and polyphenols targeted to cancer prevention. Cancers 8(6):58. https://doi.org/10.3390/cancers8060058

Martínez-Valdivieso D, Font R, Blanco-Díaz MT, Moreno-Rojas JM, Gómez P, Alonso-Moraga Á, Del Río-Celestino M (2014) Application of near-infrared reflectance spectroscopy for predicting carotenoid content in summer squash fruit. Comput Electron Agric 108:71–79. https://doi.org/10.1016/j.compag.2014.07.003

Moncada GW, González Martín MI, Escuredo O, Fischer S, Míguez M (2013) Multivariate calibration by near infrared spectroscopy for the determination of the vitamin E and the antioxidant properties of quinoa. Talanta 116:65–70. https://doi.org/10.1016/j.talanta.2013.04.079

Mora-Ruiz ME, Reboredo-Rodríguez P, Salvador MD, González-Barreiro C, Cancho-Grande B, Simal-Gándara J, Fregapane G (2017) Assessment of polar phenolic compounds of virgin olive oil by NIR and mid-IR spectroscopy and their impact on quality. Eur J Lipid Sci Technol 119(1):1600099. https://doi.org/10.1002/ejlt.201600099

Nogales-Bueno J, Hernández-Hierro JM, Rodríguez-Pulido FJ, Heredia FJ (2014) Determination of technological maturity of grapes and total phenolic compounds of grape skins in red and white cultivars during ripening by near infrared hyperspectral image: a preliminary approach. Food Chem 152:586–591. https://doi.org/10.1016/j.foodchem.2013.12.030

Nordey T, Joas J, Davrieux F, Génard M, Léchaudel M (2014) Non-destructive prediction of color and pigment contents in mango peel. Sci Hortic 171:37–44. https://doi.org/10.1016/j.scienta.2014.01.025

Osborne, B. G. (2006). Near-Infrared Spectroscopy in Food Analysis. Encyclopedia of Analytical Chemistry. John Wiley & Sons, Ltd. England

Ozaki, Y., McClure, W.F. and Christy, A.A. eds., (2006). Near-infrared spectroscopy in food science and technology. John Wiley & Sons.

Pallone JAL, Caramês ET d S, Alamar PD (2018) Green analytical chemistry applied in food analysis: alternative techniques. Curr Opin Food Sci 22:115–121. https://doi.org/10.1016/j.cofs.2018.01.009

Pavia L, Lampman GM (1996) Kriz, Introduction to spectroscopy. Harcourt Brace College Publishers, New York

Peng B, Ge N, Cui L, Zhao H (2016) Monitoring of alcohol strength and titratable acidity of apple wine during fermentation using near-infrared spectroscopy. LWT Food Sci Technol 66:86–92. https://doi.org/10.1016/j.lwt.2015.10.018

Pissard A, Pierna JAF, Baeten V, Sinnaeve G, Lognay G, Mouteau A, … Lateur M (2013) Non-destructive measurement of vitamin C, total polyphenol and sugar content in apples using near-infrared spectroscopy. J Sci Food Agric 93(2):238-244. doi:https://doi.org/10.1002/jsfa.5779

Pu Y-Y, Feng Y-Z, Sun D-W (2015) Recent progress of hyperspectral imaging on quality and safety inspection of fruits and vegetables: a review. Compr Rev Food Sci Food Saf 14(2):176–188. https://doi.org/10.1111/1541-4337.12123

Rasines-Perea Z, Prieto-Perea N, Romera-Fernández M, Berrueta LA, Gallo B (2015) Fast determination of anthocyanins in red grape musts by Fourier transform mid-infrared spectroscopy and partial least squares regression. Eur Food Res Technol 240(5):897–908. https://doi.org/10.1007/s00217-014-2394-6

Reich G (2005) Near-infrared spectroscopy and imaging: basic principles and pharmaceutical applications. Adv Drug Deliv Rev 57(8):1109–1143. https://doi.org/10.1016/j.addr.2005.01.020

Revilla I, Vivar-Quintana AM, González-Martín I, Escuredo O, Seijo C (2017) The potential of near infrared spectroscopy for determining the phenolic, antioxidant, color and bactericide characteristics of raw propolis. Microchem J 134:211–217. https://doi.org/10.1016/j.microc.2017.06.006

Rizk EM, El-Kady AT, El-Bialy AR (2014) Charactrization of carotenoids (lyco-red) extracted from tomato peels and its uses as natural colorants and antioxidants of ice cream. Ann Agric Sci 59(1):53–61. https://doi.org/10.1016/j.aoas.2014.06.008

Rungpichayapichet P, Mahayothee B, Khuwijitjaru P, Nagle M, Müller J (2015) Non-destructive determination of β-carotene content in mango by near-infrared spectroscopy compared with colorimetric measurements. J Food Compos Anal 38:32–41. https://doi.org/10.1016/j.jfca.2014.10.013

Sebben JA, da Silveira Espindola J, Ranzan L, Fernandes de Moura N, Trierweiler LF, Trierweiler JO (2018) Development of a quantitative approach using Raman spectroscopy for carotenoids determination in processed sweet potato. Food Chem 245:1224–1231. https://doi.org/10.1016/j.foodchem.2017.11.086

Sekine R, Robertson EG, McNaughton D (2011) Raman, infrared and computational analysis of genistein and its methoxy derivatives. Vib Spectrosc 57(2):306–314. https://doi.org/10.1016/j.vibspec.2011.09.005

Sen I, Ozturk B, Tokatli F, Ozen B (2016) Combination of visible and mid-infrared spectra for the prediction of chemical parameters of wines. Talanta 161:130–137. https://doi.org/10.1016/j.talanta.2016.08.057

Shahidi F, Zhong Y (2015) Measurement of antioxidant activity. J Funct Foods 18 Part B:757–781. https://doi.org/10.1016/j.jff.2015.01.047

Shan J, Suzuki T, Suhandy D, Ogawa Y, Kondo N (2014) Chlorogenic acid (CGA) determination in roasted coffee beans by near infrared (NIR) spectroscopy. Eng Agric Environ Food 7(4):139–142. https://doi.org/10.1016/j.eaef.2014.08.003

Silva SD, Feliciano RP, Boas LV, Bronze MR (2014) Application of FTIR-ATR to Moscatel dessert wines for prediction of total phenolic and flavonoid contents and antioxidant capacity. Food Chem 150: 489–493. https://doi.org/10.1016/j.foodchem.2013.11.028

Skoog, D. A., Holler, F. J., & Crouch, S. R. (2017). Principles of Instrumental Analysis. 7th Edition. Cengage learning Asia Pte Ltd, Singapore

Smith, E., & Dent, G. (2019). Modern Raman spectroscopy: a practical approach. 2and edn Wiley, John Wiley & Sons. England

Su W-H, Sun D-W (2018a) Fourier transform infrared and raman and hyperspectral imaging techniques for quality determinations of powdery foods: a review. Compr Rev Food Sci Food Saf 17(1):104–122. https://doi.org/10.1111/1541-4337.12314

Su WH, Sun DW (2018b) Multispectral imaging for plant food quality analysis and visualization. Compr Rev Food Sci Food Saf 17(1): 220–239

Sun-Waterhouse D, Wadhwa SS (2013) Industry-relevant approaches for minimising the bitterness of bioactive compounds in functional foods: a review. Food Bioprocess Technol 6(3):607–627. https://doi.org/10.1007/s11947-012-0829-2

Tahir HE, Xiaobo Z, Jiyong S, Mariod AA, Wiliam T (2016a) Rapid determination of antioxidant compounds and antioxidant activity of Sudanese Karkade (Hibiscus sabdariffa L.) using near infrared spectroscopy. Food Anal Methods 9(5):1228–1236

Tahir HE, Xiaobo Z, Tinting S, Jiyong S, Mariod AA (2016b) Near-infrared (NIR) spectroscopy for rapid measurement of antioxidant properties and discrimination of Sudanese honeys from different botanical Origin. Food Anal Methods 9(9):2631–2641. https://doi.org/10.1007/s12161-016-0453-2

Tahir HE, Xiaobo Z, Xiaowei H, Jiyong S, Mariod AA (2016c) Discrimination of honeys using colorimetric sensor arrays, sensory analysis and gas chromatography techniques. Food Chem 206:37–43. https://doi.org/10.1016/j.foodchem.2016.03.032

Tahir HE, Xiaobo Z, Zhihua L, Jiyong S, Zhai X, Wang S, Mariod AA (2017) Rapid prediction of phenolic compounds and antioxidant activity of Sudanese honey using Raman and Fourier transform infrared (FT-IR) spectroscopy. Food Chem 226(Supplement C): 202–211. https://doi.org/10.1016/j.foodchem.2017.01.024

Teixeira dos Santos CA, Páscoa RNMJ, Porto PALS, Cerdeira AL, González-Sáiz JM, Pizarro C, Lopes JA (2018) Raman spectroscopy for wine analyses: a comparison with near and mid infrared spectroscopy. Talanta 186:306–314. https://doi.org/10.1016/j.talanta.2018.04.075

Tingting S, Xiaobo Z, Jiyong S, Zhihua L, Xiaowei H, Yiwei X, Wu C (2016) Determination geographical origin and flavonoids content of goji berry using near-infrared spectroscopy and chemometrics. Food Anal Methods 9(1):68–79. https://doi.org/10.1007/s12161-015-0175-x

Tondi G, Petutschnigg A (2015) Middle infrared (ATR FT-MIR) characterization of industrial tannin extracts. Ind Crop Prod 65:422–428. https://doi.org/10.1016/j.indcrop.2014.11.005

Uncu O, Ozen B (2015) Prediction of various chemical parameters of olive oils with Fourier transform infrared spectroscopy. LWT Food Sci Technol 63(2):978–984. https://doi.org/10.1016/j.lwt.2015.05.002

Viegas TR, Mata ALML, Duarte MML, Lima KMG (2016) Determination of quality attributes in wax jambu fruit using NIRS and PLS. Food Chem 190:1–4. https://doi.org/10.1016/j.foodchem.2015.05.063

Williams PC, Stevensen SG (1990) Near-infrared reflectance analysis: food industry applications. Trends Food Sci Technol 1:44–48. https://doi.org/10.1016/0924-2244(90)90030-3

Wojciechowski C, Dupuy N, Ta CD, Huvenne JP, Legrand P (1998) Quantitative analysis of water-soluble vitamins by ATR-FTIR spectroscopy. Food Chem 63(1):133–140. https://doi.org/10.1016/S0308-8146(97)00138-6

Wu Z, Xu E, Long J, Pan X, Xu X, Jin Z, Jiao A (2016) Comparison between ATR-IR, Raman, concatenated ATR-IR and Raman spectroscopy for the determination of total antioxidant capacity and total phenolic content of Chinese rice wine. Food Chem 194:671–679. https://doi.org/10.1016/j.foodchem.2015.08.071

Xia, F., Li, C., Zhao, N., Li, H., Chang, Q., Liu, X., … Pan, R. (2018). Rapid determination of active compounds and antioxidant activity of okra seeds using Fourier transform near infrared (FT-NIR) spectroscopy. Molecules 23(3):550.

Xiaowei H, Xiaobo Z, Jiewen Z, Jiyong S, Xiaolei Z, Holmes M (2014) Measurement of total anthocyanins content in flowering tea using near infrared spectroscopy combined with ant colony optimization models. Food Chem 164:536–543. https://doi.org/10.1016/j.foodchem.2014.05.072

Yahui L, Xiaobo Z, Tingting S, Jiyong S, Jiewen Z, Holmes M (2017) Determination of geographical origin and anthocyanin content of black goji berry (Lycium ruthenicum Murr.) Using near-infrared spectroscopy and chemometrics. Food Anal Methods 10(4):1034–1044. https://doi.org/10.1007/s12161-016-0666-4

Yang H, Irudayaraj J (2002) Rapid determination of vitamin c by NIR, MIR and FT-Raman techniques. J Pharm Pharmacol 54(9):1247–1255. https://doi.org/10.1211/002235702320402099

Yang Y-C, Sun D-W, Pu H, Wang N-N, Zhu Z (2015) Rapid detection of anthocyanin content in lychee pericarp during storage using hyperspectral imaging coupled with model fusion. Postharvest Biol Technol 103:55–65. https://doi.org/10.1016/j.postharvbio.2015.02.008

Zhang N, Liu X, Jin X, Li C, Wu X, Yang S, Ning J, Yanne P (2017) Determination of total iron-reactive phenolics, anthocyanins and tannins in wine grapes of skins and seeds based on near-infrared hyperspectral imaging. Food Chem 237:811–817. https://doi.org/10.1016/j.foodchem.2017.06.007

Žilić S, Janković M, Basić Z, Vančetović J, Maksimović V (2016) Antioxidant activity, phenolic profile, chlorophyll and mineral matter content of corn silk (Zea mays L): comparison with medicinal herbs. J Cereal Sci 69:363–370. https://doi.org/10.1016/j.jcs.2016.05.003